

Left-right supersymmetry after the Higgs discovery

Mariana Frank,^a Dilip Kumar Ghosh,^b Katri Huitu,^c Santosh Kumar Rai,^d Ipsita Saha,^b Harri Waltari^c

^a*Department of Physics, Concordia University, 7141 Sherbrooke St. West, Montreal, Quebec, Canada H4B 1R6,*

^b*Department of Theoretical Physics, Indian Association for the Cultivation of Science, 2A & 2B Raja S.C. Mullick Road, Kolkata 700 032, India,*

^c*Department of Physics and Helsinki Institute of Physics, P.O. Box 64 (Gustaf H  llstr  min katu 2), FIN-00014 University of Helsinki, Finland,*

^d*Regional Centre for Accelerator-based Particle Physics, Harish-Chandra Research Institute, Chhatnag Road, Jhusi, Allahabad 211019, India.*

E-mail: mariana.frank@concordia.ca, tpdkg@iacs.res.in,
katri.huitu@helsinki.fi, skrai@hri.res.in, tpis@iacs.res.in,
harri.waltari@helsinki.fi

ABSTRACT: We perform a thorough analysis of the parameter space of the minimal left-right supersymmetric model in agreement with the LHC data. The model contains left- and right-handed fermionic doublets, two Higgs bidoublets, two Higgs triplet representations, and one singlet, insuring a charge-conserving vacuum. We impose the condition that the model complies with the experimental constraints on supersymmetric particles masses and on the doubly-charged Higgs bosons, and require that the parameter space of the model satisfy the LHC data on neutral Higgs signal strengths at 2σ . We choose benchmark scenarios by fixing some basic parameters and scanning over the rest. The LSP in our scenarios is always the lightest neutralino. We find that the signals for $H \rightarrow \gamma\gamma$ and $H \rightarrow VV^*$ are correlated, while $H \rightarrow b\bar{b}$ is anti-correlated with all the other decay modes, and also that the contribution from singly-charged scalars dominate that of the doubly-charged scalars in $H \rightarrow \gamma\gamma$ and $H \rightarrow Z\gamma$ loops, contrary to Type-II seesaw models. We also illustrate the range for mass spectrum of the LRSUSY model in light of planned measurements of the branching ratio of $H \rightarrow \gamma\gamma$ to 10% level.

KEYWORDS: LHC phenomenology, Left Right Symmetry, Supersymmetry

Contents

1	Introduction	1
2	The Higgs sector of the left-right supersymmetric model	3
3	The Supersymmetric Spectrum	8
3.1	Charginos	9
3.2	Neutralinos	11
3.3	Sleptons	12
4	The decay modes of H_1^0	13
4.1	$H_1^0 \rightarrow \gamma\gamma$	13
4.2	$H_1^0 \rightarrow Z\gamma$	14
4.3	$H_1^0 \rightarrow XX$	15
5	Implications for model parameters	15
6	Conclusions	24

1 Introduction

The discovery of the Higgs boson at the LHC [1, 2] highlighted the importance of the search for signs for Beyond the Standard Model (BSM) in the Higgs boson decay or production modes. While the amount of data at LHC with $\sqrt{s} = 7$ and 8 TeV is still rather limited, if combined with the measured Higgs mass, it seems to fit very well the Standard Model (SM) predictions and thus it allows one to restrict the parameter space of many BSM models. In the SM, the Higgs signal rates (cross section times branching ratios) are completely fixed by the Higgs mass. Precise predictions for decays into various channels can be combined with the experimental data to define a signal strength for each decay μ_i , normalized such that the SM corresponds to $\mu_i = 1$. The mass of the Higgs boson is measured using the decay modes with clear mass peaks, $H \rightarrow ZZ^* \rightarrow 4\ell$ and $H \rightarrow \gamma\gamma$ [3, 4]. Other decay modes of Higgs into WW^* , $b\bar{b}$, and $\tau^+\tau^-$ has been measured both by CMS and ATLAS [1, 2]. For recent updates in these channels we refer to [5–7].

There are two ways in which a non-minimal BSM Higgs sector could be revealed experimentally: either directly through the discovery of additional scalar states, or through precise measurements of the Higgs properties, that would indicate deviations from the SM predictions for the scalar state discovered at 126 GeV. At present, the only measurement in the Higgs sector, which, within the accuracy of measurement, seems to possibly differ from the SM prediction, is the di-photon mode as measured by the ATLAS [5] and CMS [6, 7]

Collaborations. Consequently, there has been a lot of recent work on the decay rate of the Higgs boson to two photons.

One approach would be to fit the data in a model-independent way [8–11]. One could also evaluate Higgs decays in specific BSM scenarios, which lead to the modifications of the Higgs couplings, especially for cases where additional particles which interact with the Higgs boson exist, and/or where there is an extended Higgs sector. In the Standard Model the dominant contribution to the decay $H \rightarrow \gamma\gamma$ is given by the interference between the top quarks and the W-boson contributions at one-loop level. In a number of possible frameworks for BSM physics, many more particles are present in the loop, and their contribution can interfere either constructively or destructively with the loops containing the SM particles. The quest for the identity of the particle discovered at the LHC has thus taken the approach of focusing on a specific new Higgs model, including models with extended gauge and/or Higgs sector and exotic particles, without supersymmetry [12–20], in MSSM or extended supersymmetric models [21–24], or in extra-dimensional models [25]. In addition, the effects of BSM physics can appear in the changes of partial widths of other known Higgs decay modes. Already, a small change in the dominant decay mode to b -quarks can significantly change the di-photon rate. The BSM models can also generate new decay modes of Higgs bosons, *e.g.* an invisible decay mode, possible in some models and experimentally allowed.

On fundamental theoretical grounds, it is expected that the Standard Model is not the final theory, and supersymmetric models remain good candidates for realistic BSM models. The minimal supersymmetric standard model (MSSM), favored because it is the simplest supersymmetric extension of the SM, is by far the most studied version of the supersymmetric models. However, in view of the LHC measurements, it is itself somewhat fine tuned, and it inherits some of the limitations of the SM as well, such as the absence of neutrino masses. In particular, one imposes by hand a discrete symmetry, R -parity, to prevent the fast decay of proton without invoking very small Yukawa-type couplings. This can be cured by including in the gauge group a part which automatically takes care of the conservation of R -parity, $R_p = (-1)^{B-L+2s}$, where B is the baryon number, L is the lepton number, and s is spin. Every model which contains $U(1)_{B-L}$ as part of the gauge symmetry, conserves R -parity at the Lagrangian level, and thus it can be only spontaneously broken, if at all.

Left-right supersymmetric (LRSUSY) models are based on enlarging the SM symmetry to the $SU(3)_c \otimes SU(2)_L \otimes SU(2)_R \otimes U(1)_{B-L}$ gauge group [26–28]. The models emerge from breaking of gauge unification scenarios such as $SO(10)$ or E_6 [29–33], or as custodial symmetry in extra-dimensional models, in particular the warped space models [34, 35]. The LRSUSY models can contain triplet scalars, which by interacting with leptons generate masses for neutrinos via seesaw mechanism [36]. The measured oscillations [37, 38] between neutrino generations would not be possible without nonzero mass of the neutrinos, which can be taken as an experimental evidence for the BSM physics. The LRSUSY model also resolves some other problems plaguing the MSSM, *e.g.* a solution to the strong and electroweak (EW) CP problems [39–42]. The triplet Higgs representations in the LRSUSY model contain both singly and doubly charged scalars and higgsinos, which would be expected to modify the di-photon rate compared to the Standard Model.

It is our aim in this paper to study the Higgs sector, in particular the relationship between the mass parameters, supersymmetric spectrum and Higgs decay widths of the model. Our aim is two-fold: to show that the model can allow an enhancement of the Higgs branching ratio into two photons, and at the same time agree with the limits on other decay modes. Our second goal is, based on the analysis of the Higgs sector, to restrict and/or make some general predictions about the parameter space of LRSUSY models. Our work is organized as follows. After reviewing in Sec. 2 the parts of the model relevant for our purposes, we study the spectrum of the model in Sec. 3. In Sec. 4 we study the rare decay modes $H \rightarrow \gamma\gamma, Z\gamma$ to see if the corresponding branching ratios differ from the SM. In Sec. 5 we consider the restriction to the parameter space, and finally we conclude in Sec. 6.

2 The Higgs sector of the left-right supersymmetric model

Left-right supersymmetric models are based on enlarging the SM symmetry to the $SU(3)_c \otimes SU(2)_L \otimes SU(2)_R \otimes U(1)_{B-L}$ gauge group [26–28].

The chiral (matter) sector of the theory contains left-handed (Q_L and L_L) and right-handed (Q_R and L_R) doublets of quark and lepton supermultiplets,

$$\begin{aligned} (Q_L)^i &= \begin{pmatrix} u_L^i \\ d_L^i \end{pmatrix} = (\mathbf{3}, \mathbf{2}, \mathbf{1}, \frac{1}{3}) , & (Q_R)_i &= \begin{pmatrix} u_{Ri}^c & d_{Ri}^c \end{pmatrix} = (\bar{\mathbf{3}}, \mathbf{1}, \mathbf{2}^*, -\frac{1}{3}) , \\ (L_L)^i &= \begin{pmatrix} \nu_L^i \\ \ell_L^i \end{pmatrix} = (\mathbf{1}, \mathbf{2}, \mathbf{1}, -1) , & (L_R)_i &= \begin{pmatrix} \nu_{Ri}^c & \ell_{Ri}^c \end{pmatrix} = (\mathbf{1}, \mathbf{1}, \mathbf{2}^*, 1) , \end{aligned} \quad (2.1)$$

where the i is a generation index, \mathbf{c} denotes charge conjugation, and, for simplicity, we have suppressed color indices.

The gauge sector of the theory includes gauge and gaugino fields, corresponding to the four gauge groups:

$$\begin{aligned} SU(3)_c : V_c &= (\mathbf{8}, \mathbf{1}, \mathbf{1}, 0) \equiv (g_\mu^a, \tilde{g}^a) , \\ SU(2)_L : V_{2L} &= (\mathbf{1}, \mathbf{3}, \mathbf{1}, 0) \equiv (W_{L\mu}^k, \tilde{W}_L^k) , \\ SU(2)_R : V_{2R} &= (\mathbf{1}, \mathbf{1}, \mathbf{3}, 0) \equiv (W_{R\mu}^k, \tilde{W}_R^k) , \\ U(1)_{B-L} : V_{B-L} &= (\mathbf{1}, \mathbf{1}, \mathbf{1}, 0) \equiv (B_\mu, \tilde{B}) . \end{aligned} \quad (2.2)$$

The $SU(3)_c \otimes SU(2)_L \otimes SU(2)_R \otimes U(1)_{B-L}$ gauge group is broken down to the Standard Model gauge group via a set of two $SU(2)_R$ Higgs triplets Δ^c and $\bar{\Delta}^c$, which are evenly charged under the $B - L$ gauge symmetry¹. Often, in non-minimal models, extra $SU(2)_L$ Higgs triplets Δ and $\bar{\Delta}$ are introduced to preserve parity at higher scales. Unfortunately, with the triplet representation, the minimum of the scalar potential is charge-violating, unless the right-chiral scalar neutrinos get vacuum expectation values (vevs), breaking R -parity spontaneously [42, 43].

Three scenarios have been proposed which remedy this situation. First, to avoid R -parity violation, in Refs. [44, 45] non-renormalizable operators are introduced at Planck

¹Doublets are also possible, but triplets are preferred as they facilitate the seesaw mechanism for neutrino mass generation [36].

scale, which shift the minimum of the potential. Second, in Refs. [46, 47], an additional singlet chiral supermultiplet (S) is added to the field content of the model, leading, after including one-loop Coleman-Weinberg corrections, to an R -parity conserving minimum of the scalar potential. And third, in Refs. [48, 49], two extra Higgs triplets $\Sigma_1 = (\mathbf{1}, \mathbf{3}, \mathbf{1}, 0)$ and $\Sigma_2 = (\mathbf{1}, \mathbf{1}, \mathbf{3}, 0)$ are included, yielding symmetry breaking with conserved R -parity at tree-level. In this work we adopt the second approach as the minimal solution. The breaking of the $SU(2)_L \otimes U(1)_Y$ symmetry to $U(1)_{\text{EM}}$ is achieved with two $SU(2)_L \otimes SU(2)_R$ Higgs bidoublets Φ_1 and Φ_2 which also generate non-trivial quark mixing angles [50]. The field content of the Higgs sector is thus summarized as

$$\begin{aligned}\Phi_1 &= \begin{pmatrix} \phi_1^0 & \phi_2^+ \\ \phi_1^- & \phi_2^0 \end{pmatrix} = (\mathbf{1}, \mathbf{2}, \mathbf{2}^*, 0), & \Phi_2 &= \begin{pmatrix} \chi_1^0 & \chi_2^+ \\ \chi_1^- & \chi_2^0 \end{pmatrix} = (\mathbf{1}, \mathbf{2}, \mathbf{2}^*, 0), \\ \Delta^c &= \begin{pmatrix} \frac{\delta^{c-}}{\sqrt{2}} & \delta^{c0} \\ \delta^{c--} & -\frac{\delta^{c-}}{\sqrt{2}} \end{pmatrix} = (\mathbf{1}, \mathbf{1}, \mathbf{3}, -2), & \bar{\Delta}^c &= \begin{pmatrix} \frac{\bar{\delta}^{c+}}{\sqrt{2}} & \bar{\delta}^{c++} \\ \bar{\delta}^{c0} & -\frac{\bar{\delta}^{c+}}{\sqrt{2}} \end{pmatrix} = (\mathbf{1}, \mathbf{1}, \mathbf{3}, 2), \\ S &= (\mathbf{1}, \mathbf{1}, \mathbf{1}, 0).\end{aligned}\tag{2.3}$$

The superpotential describing the interactions among the chiral supermultiplets of the model is

$$\begin{aligned}W(\phi) &= (Q_L)^i Y_Q^1(\Phi_1)(Q_R)_i + (Q_L)^i Y_Q^2(\Phi_2)(Q_R)_i + (L_L)^i Y_L^1(\Phi_1)(L_R)_i + (L_L)^i Y_L^2(\Phi_2)(L_R)_i \\ &\quad + i(L_R)_i f(\Delta^c)(L_R)^i + S [\lambda \text{Tr}(\Delta^c \cdot \bar{\Delta}^c) - \mathcal{M}_R^2] + \lambda_{12} S \text{Tr}(\Phi_1 \cdot \Phi_2)\end{aligned}$$

where i is a generation index, Y_Q^j, Y_L^j ($j = 1, 2$), and f are 3×3 matrix Yukawa couplings.

The full scalar potential of the model, which is minimized to obtain the masses and composition of the Higgs bosons, is given by

$$\begin{aligned}V_F &= \left| \lambda \text{Tr}(\Delta^c \bar{\Delta}^c) + \lambda_{12} \text{Tr}(\Phi_1^T \Phi_2) - \mathcal{M}_R^2 \right|^2 + \lambda^2 |S|^2 \left| \text{Tr}(\Delta^c \Delta^{c\dagger}) + \text{Tr}(\bar{\Delta}^c \bar{\Delta}^{c\dagger}) \right|, \\ V_{\text{soft}} &= M_1^2 \text{Tr}(\Delta^{c\dagger} \Delta^c) + M_2^2 \text{Tr}(\bar{\Delta}^{c\dagger} \bar{\Delta}^c) + M_3^2 \Phi_1^\dagger \Phi_1 + M_4^2 \Phi_2^\dagger \Phi_2 + M_S^2 |S|^2 \\ &\quad + \{A_\lambda \lambda S \text{Tr}(\Delta^c \bar{\Delta}^c) - C_\lambda \mathcal{M}_R^2 S + h.c.\}, \\ V_D &= \frac{g_L^2}{8} \sum_i \left| \text{Tr}(\Phi_1 \Phi_2^\dagger) \right|^2 + \frac{g_R^2}{8} \sum_i \left| \text{Tr}(2\Delta^{c\dagger} \Delta^c + 2\bar{\Delta}^{c\dagger} \bar{\Delta}^c + \Phi_1 \Phi_2^\dagger) \right|^2 \\ &\quad + \frac{g_{B-L}^2}{2} \left| \text{Tr}(-\Delta^{c\dagger} \Delta^c + \bar{\Delta}^{c\dagger} \bar{\Delta}^c) \right|^2.\end{aligned}\tag{2.4}$$

The gauge symmetry is spontaneously broken in two steps. First the $SU(2)_R \otimes U(1)_{B-L}$ gauge group is broken to the SM gauge group, which is subsequently broken to the electromagnetic group $U(1)_{\text{EM}}$ by the vacuum expectation values (VEVs) of the neutral components of the Higgs fields

$$\begin{aligned}\langle S \rangle &= \frac{v_s}{\sqrt{2}} e^{i\alpha_s}, & \langle \Phi_1 \rangle &= \begin{pmatrix} \frac{v_1}{\sqrt{2}} & 0 \\ 0 & \frac{v'_1}{\sqrt{2}} e^{i\alpha_1} \end{pmatrix}, & \langle \Phi_2 \rangle &= \begin{pmatrix} \frac{v'_2}{\sqrt{2}} e^{i\alpha_2} & 0 \\ 0 & \frac{v_2}{\sqrt{2}} \end{pmatrix}, \\ \langle \Delta^c \rangle &= \begin{pmatrix} 0 & \frac{v_R}{\sqrt{2}} \\ 0 & 0 \end{pmatrix}, & \langle \bar{\Delta}^c \rangle &= \begin{pmatrix} 0 & 0 \\ \frac{\bar{v}_R}{\sqrt{2}} & 0 \end{pmatrix}.\end{aligned}\tag{2.5}$$

The VEVs $v_R, \bar{v}_R, v_1, v_2, v'_1, v'_2$ and v_s can be chosen real and non-negative, while the only complex phases which cannot be rotated away by means of suitable gauge transformations and field redefinitions are denoted by explicit angles α_1, α_2 and α_s . However, as the CP -violating $W_L^\pm - W_R^\pm$ mixing is proportional to $v_1 v'_1 e^{i\alpha_1}$ and $v_2 v'_2 e^{i\alpha_2}$, and is constrained to be small by $K^0 - \bar{K}^0$ mixing data, this forces the angles to be very small. As the number of degrees of freedom remains large, we assume the hierarchy

$$v_R, \bar{v}_R \gg v_2, v_1 \gg v'_1 = v'_2 \approx 0 \quad \text{and} \quad \alpha_1 = \alpha_2 = \alpha_s \approx 0. \quad (2.6)$$

The minimization of the scalar potential yields an R -parity violating, or a charge violating, vacuum. The simplest and most efficient way to avoid either is to introduce one-loop Coleman-Weinberg effective potential terms, generated by right-chiral leptons coupling to the Δ^c field:

$$V_{\text{eff}}^{1\text{-loop}} = \frac{1}{16\pi^2} \sum_i (-1)^{2s} (2s+1) M_i^4 \left[\ln \left(\frac{M_i^2}{\mu^2} \right) - \frac{3}{2} \right] \quad (2.7)$$

Expanding this potential in the limit in which the SUSY breaking parameters are small with respect to the triplet VEVs (v_R, \bar{v}_R), one obtains an effective form of the potential in terms of the small parameter:

$$x = \frac{\text{Tr}(\Delta^c \Delta^c) \text{Tr}((\Delta^{c\dagger} \Delta^{c\dagger}))}{[\text{Tr}(\Delta^{c\dagger} \Delta^c)]^2}.$$

To lowest order in x , the effective quadratic term in the one-loop potential becomes:

$$V_{\text{quad.}}^{1\text{-loop}} \simeq - \frac{|f|^2 (M_{\bar{l}})_R^2 \text{Tr}(\Delta^c \Delta^c) \text{Tr}(\Delta^{c\dagger} \Delta^{c\dagger})}{128\pi^2 |v_R|^2} \left\{ (a_1 - a_2) g_R^2 \left(2 \ln \frac{|f v_R|^2}{\mu^2} + \ln x - 2 \ln 2 - 2 \right) - [2 + (a_1 + a_2) g_{B-L}^2] (\ln x - 2 \ln 2) \right\} \quad (2.8)$$

Here a_1 and a_2 correction terms which vanish in the SUSY limit (when D -terms vanish) and $(M_{\bar{l}})_R$ are soft right-handed scalar lepton masses. Before introducing the one-loop corrections, the global minimum contained at least one doubly-charged Higgs boson with zero or negative mass, but after one-loop corrections all the masses are positive and the masses become very predictive.

The Higgs boson spectrum of this model was previously analyzed in [47], which included constraints from FCNC processes from $\epsilon_K, K^0 - \bar{K}^0, D^0 - \bar{D}^0$ and $B_{d,s}^0 - \bar{B}_{d,s}^0$ data. Here we re-evaluate the masses and mixings to account for the lightest CP-even Higgs boson with a mass of ~ 125 GeV, and to obey restrictions on the spectrum arising from recent constraints on the other Higgs boson masses. We review these below.

For the doubly charged Higgs bosons, the most up-to-date mass bounds have been obtained through the direct searches at the LHC. The ATLAS Collaboration has looked for doubly charged Higgs bosons in pair production of same sign di-lepton final states. Based on the data sample corresponding to an integrated luminosity of 4.7 fb^{-1} at $\sqrt{s} = 7$ TeV, masses below 409 GeV, 375 GeV and 398 GeV have been excluded for $e^\pm e^\pm, e^\pm \mu^\pm$ and $\mu^\pm \mu^\pm$, respectively, assuming a branching ratio of 100% for each final state [51]. The CMS Collaboration also searched for the pair production $pp \rightarrow H^{\pm\pm} H^{\mp\mp}$ and for the

associated production $pp \rightarrow H^{\pm\pm} H^\mp$, in which the masses of $H^{\pm\pm}$ and H^\mp are assumed to be degenerate. Using three or more isolated charged lepton final states, the lower limit on $M_{H^{\pm\pm}}$ was found to be between 204 and 459 GeV in the 100% branching fraction scenarios. Specifically, for $e^\pm e^\pm$, $e^\pm \mu^\pm$, $e^\pm \tau^\pm$, $\mu^\pm \mu^\pm$, $\mu^\pm \tau^\pm$, and $\tau^\pm \tau^\pm$, the 90 % C.L. limits obtained are 444 GeV, 453 GeV, 373 GeV, 459 GeV, 375 GeV, and 204 GeV respectively [52]. In our work we assume that the decay $H^{\pm\pm} \rightarrow \tau^\pm \tau^\pm$ dominates, while the others are negligible, allowing the lower limit of the doubly charged Higgs boson mass to be consistent with LHC searches.

In LRSUSY the tree-level contribution for the lightest CP-even scalar mass is given by $\frac{1}{2}\sqrt{g_L^2 + g_R^2} v |\cos 2\beta|$ [53]. Since we do not include left-handed triplets, we can treat g_R as a free parameter. If we assume $g_R = g_L$ (at the electroweak scale) the tree-level mass bound is lifted to 113 GeV, so the radiative corrections needed for a 125 GeV Higgs are much smaller than in the MSSM. The tree-level mass bound has an effect on the allowed range of $\tan\beta$. The radiative corrections depend mostly on stop and sbottom masses. If we fix the third generation squark masses, there will be a lower bound on the value of $\tan\beta$. For the squark masses in our scans the allowed range is $\tan\beta > 6$. If the squarks are assumed to be heavier, the bound on $\tan\beta$ will become weaker.

Fixed Parameters	BP1	BP2	BP3
M_1	250	150	250
M_{2L}	500	200	500
M_{2R}	500	200	500
M_3	1500	1500	1500
v_s	2000	2000	2000
Y_ν	0.00003	0.00003	0.00003
$(M_{H^{\pm\pm}})_{min}$	200.0	200.0	200.0
$(M_A)_{min}$	300.0	300.0	300.0

Table 1: Fixed input parameters for the LRSUSY model. The masses are in GeV.

We show three benchmark points for the parameters of the LRSUSY model. We fix gaugino masses, the singlet VEV, the neutrino Yukawa coupling, the doubly charged and pseudoscalar Higgs masses as shown in Table 1. The last five parameters mentioned are the same for all benchmarks.

As we wish to study the two-photon decay channel, which is influenced by all charged particles, the benchmark scenarios are designed to make some of the charged particles light. The doubly charged Higgs is light in all benchmarks. In BP2 we have light charginos and in BP3 we have light staus.

In Table 2, we show the parameters on which the scanning is done. Note that the BP1 and BP3 benchmarks have the same gaugino masses, but are differentiated by running over different soft right-handed slepton masses (heavier in BP1, lighter in BP3 benchmarks).

The lightest CP-even state in our model (with mass $M_{H_1^0} \sim 125$ GeV) is SM-like, that is, it is composed mainly of Higgs bidoublet components. The next lightest state is

Parameter	BP1		BP2		BP3	
	Minimum	Maximum	Minimum	Maximum	Minimum	Maximum
$\tan\beta$	2.5	40	2.5	40	2.5	40
λ	0.3	0.6	0.3	0.6	0.3	0.6
$(M_{\tilde{q}})_L(\text{GeV})$	1000	1500	1000	1500	1000	1500
$(M_{\tilde{q}})_R(\text{GeV})$	1000	1500	1000	1500	1000	1500
$(M_{\tilde{l}})_L(\text{GeV})$	1000	1500	1000	1500	100	300
$(M_{\tilde{l}})_R(\text{GeV})$	1000	1500	1000	1500	500	700
f	0.4	0.7	0.4	0.7	0.55	0.7
$M_R(\text{GeV})$	100000	150000	100000	150000	100000	150000
A	-2000	2000	-2000	2000	-2000	2000
$\mu_{eff}(\text{GeV})$	-700	-400	-500	-200	-700	-400
$v_R(\text{GeV})$	4000	5000	4000	5000	3000	4500
$\tan\delta$	0.93	0.99	0.93	0.99	0.96	0.99

Table 2: Ranges of the input parameters in the scan used to compute the Higgs production and decays for the BP1, BP2 and BP3 benchmarks.

the doubly charged Higgs boson $H_1^{\pm\pm}$. Its mass varies in the 200-300 GeV region, and is sensitive to the ratio of the two triplet Higgs VEVs, $\tan\delta = \frac{\bar{v}_R}{v_R}$, the soft mass for the right-handed sleptons $(M_{\tilde{l}})_R$, and the triplet Higgs Yukawa coupling, f . We show these variations in the plots in Fig. 1. We note that no masses for the doubly charged Higgs boson are obtained if $\tan\delta$ increases beyond 0.983. The values of $\tan\delta$ are restricted by the experimental bounds for the lightest CP-odd scalar and the charged Higgs masses, as shown in Fig. 2. If the limit on these masses is relaxed, points satisfying the doubly charged mass limit can be obtained with $\tan\delta$ values close to one. The scans are performed in the range $0.93 < \tan\delta < 0.99$. At the lower end it becomes more difficult to satisfy the bound on the

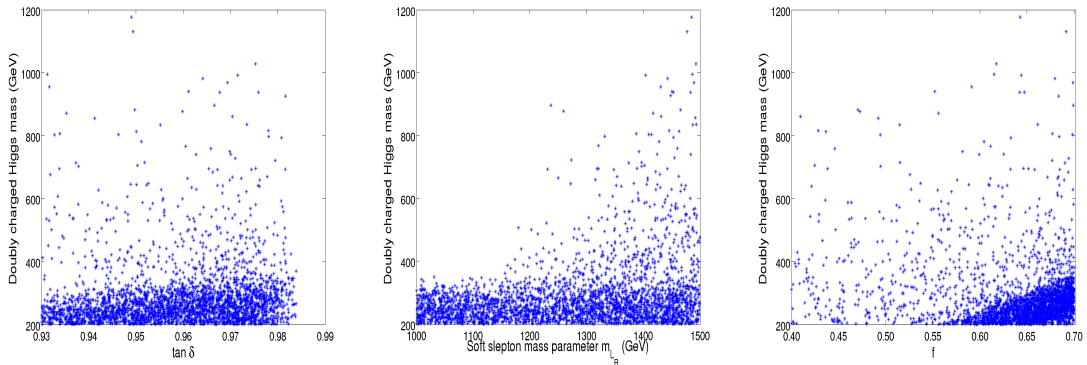


Figure 1: Dependence of the mass of the doubly charged Higgs boson on the parameters of the model, as given in the Table 2. We show the variation with $\tan\delta$, the soft mass for the right-handed m_{LR} , and the triplet Higgs Yukawa coupling, f .

doubly charged Higgs mass. This is due to the fact that the diagonal elements of the doubly charged Higgs mass matrix have terms $\pm 2g_R^2(v_R^2 - \bar{v}_R^2)$ [47]. Hence if $\tan \delta$ deviates largely from one, one of these values will become increasingly negative and hence larger radiative corrections are needed to satisfy the bound on the doubly charged Higgs mass. With the range we use for v_R , the doubly charged Higgs mass constraint requires $\tan \delta > 0.9$ and there are very few points which survive the 200 GeV constraint in the lower end of the range. On the other hand it is not possible to have smaller values of v_R since that would result in a too low a W_R mass.

The doubly charged Higgs mass depends on the soft right-handed slepton mass, as in Eq. 2.8, since this parameter determines the amount of supersymmetry breaking in the $\tau - \tilde{\tau}$ loops. However, masses in the 200-300 GeV region are obtained for all values $(M_{\tilde{l}})_R$ in the 1-1.5 TeV region; while heavier masses are more likely for heavier slepton masses. The most striking impact on the doubly charged Higgs mass comes from the parameter f , the Yukawa coupling for the triplet Higgs bosons, which is the coefficient of the term that gives radiative corrections from $\tau - \tilde{\tau}$ loops to the doubly charged Higgs mass. While parameter points with $f \in (0.4, 0.6)$ range exist, the experimental constraints on the doubly charged Higgs mass clearly favor large triplet Yukawa couplings, $f > 0.6$ for soft slepton masses around 1 TeV. For larger soft slepton masses one can get viable doubly charged Higgs masses with smaller values of f also. The other radiative contributions to the doubly charged Higgs mass come from the singlet Higgs loops, but that contribution is large only if we let the effective μ -parameter be in the TeV range. This will lead to fine tuning in the Z boson mass. The second lightest CP-even Higgs boson is predicted to be relatively light². This Higgs boson is also mostly doublet-like: we show its composition in the left-hand upper panel of Fig. 2, where it is seen that the triplet components are negligible. The dependence of its mass with $\tan \delta$ (upper right-hand panel), with the mass of the lightest singly charged Higgs boson (lower left-hand panel), and with the mass of the lightest pseudoscalar (lower right-hand panel) is almost linear. A heavier neutral Higgs favors $\tan \delta \sim 0.93$, while the mass splittings between the second lightest CP-even neutral Higgs and the lightest singly charged Higgs, as well as the pseudoscalar, are $M_{H_2^0} - M_{H_1^\pm} \sim M_{H_2^0} - M_A \lesssim 50$ GeV. The average compositions and masses of the lightest Higgs bosons are shown in Table 3.

3 The Supersymmetric Spectrum

First, we assume that squarks and gluinos are heavy, in agreement with the LHC limits. Direct searches for squarks and gluinos require their soft mass terms to be at least at TeV scale. Squark masses below 780 GeV and gluino masses of up to 1.1–1.2 TeV are excluded at 95% CL within several models, for LSP masses below 100 GeV at CMS [54]. The third generation squark masses need to be large also to generate the radiative corrections to the Higgs mass. In contrast, neutralinos [55], charginos and sleptons [56] are still allowed to be lighter.

The mass spectrum of the lightest superpartners is largely determined by the soft supersymmetry breaking parameters. Since they are in principle unknown, there are for

²This is the second FCNC-conserving neutral Higgs boson.

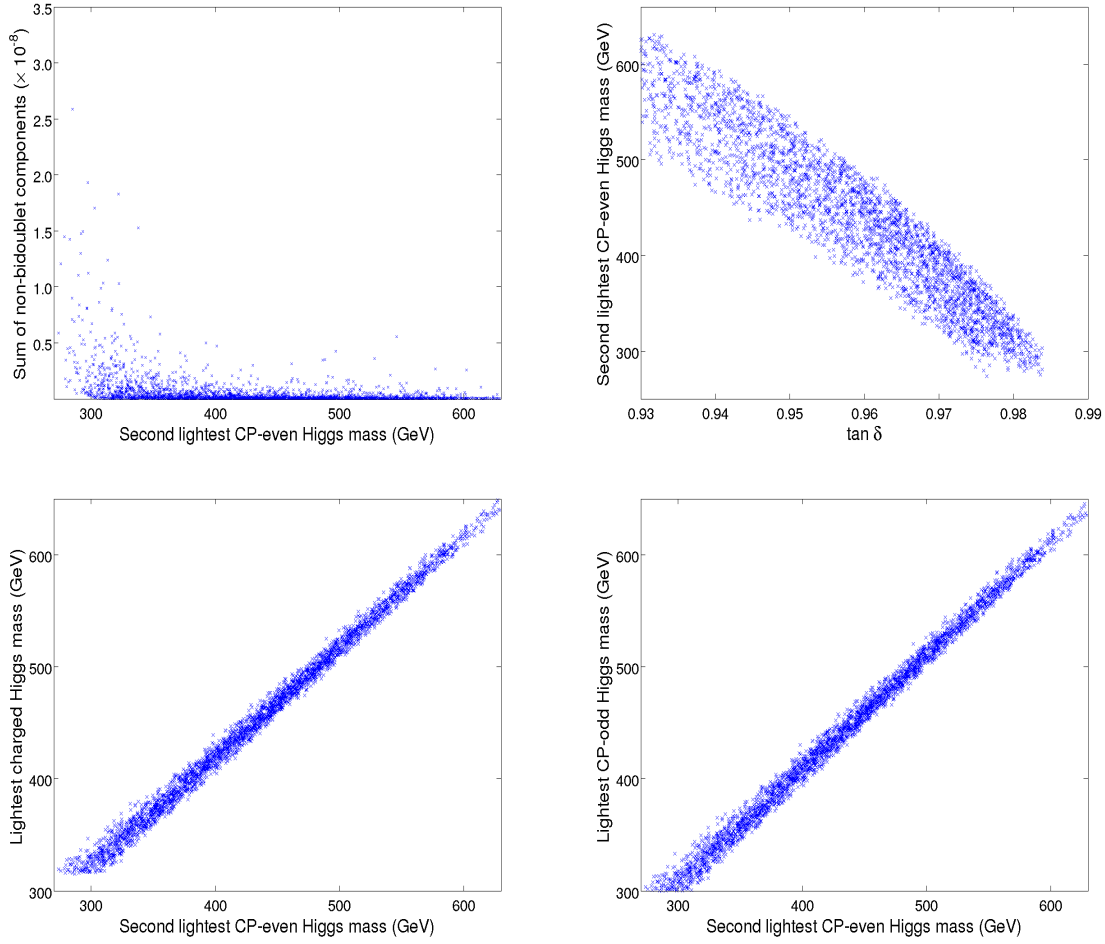


Figure 2: Dependence of the mass of the second lightest CP-even Higgs boson on the parameters of the model, as given in the Table 2. We show the triplet composition of the state (upper left panel), the variation with $\tan \delta$ (upper right panel), dependence on the lightest singly charged Higgs mass M_{H^\pm} (lower left panel) and on the lightest pseudoscalar mass M_A (lower right panel).

instance several viable alternatives for the LSP. The different options for dark matter in LRSUSY have been studied in [57, 58].

3.1 Charginos

In this model there are five singly charged charginos, which can be given in the following basis $(\tilde{\Delta}^\pm, \tilde{\Phi}_1^\pm, \tilde{\Phi}_2^\pm, \tilde{W}_L^\pm, \tilde{W}_R^\pm)$. The mass matrix is

Component	H_1^0	H_2^0	H_3^0	Component	H_1^+	H_1^{++}
ϕ_1^0	99.65%	0.01%	—	ϕ_1^+	99.58%	
ϕ_2^0	0.01%	99.65%	—	χ_1^+	0.34%	
χ_1^0	—	0.34%	—	δ^{c+}	0.04%	
χ_2^0	0.34%	—	—	$\bar{\delta}^{c+}$	0.04%	
δ^{c0}	—	—	52.10%	δ^{c++}		52.11%
$\bar{\delta}^{c0}$	—	—	47.90%	$\bar{\delta}^{c++}$		47.89%
Mass (GeV)	123.5	436.3	1988		455.4	286.8

Table 3: The average compositions and masses of the lightest Higgs bosons for benchmark BP1. For benchmark BP2 the results are similar except for the mass of H_3^0 , which is 2280 GeV. For benchmark BP3 the compositions are similar but the masses are somewhat lighter: 351.0 GeV (H_2^0), 1818 GeV (H_3^0), 370.3 GeV (H_1^+) and 238.7 GeV (H_1^{++}).

$$M_{\tilde{\chi}^\pm} = \begin{pmatrix} \lambda v_s/\sqrt{2} & 0 & 0 & 0 & -g_R v_R \\ 0 & 0 & \mu_{\text{eff}} & g_L v_u/\sqrt{2} & 0 \\ 0 & \mu_{\text{eff}} & 0 & 0 & -g_R v_d/\sqrt{2} \\ 0 & 0 & g_L v_d/\sqrt{2} & M_{2L} & 0 \\ g_R \bar{v}_R & -g_R v_u/\sqrt{2} & 0 & 0 & M_{2R} \end{pmatrix} \quad (3.1)$$

The mass spectrum essentially depends on M_{2L} , M_{2R} , μ_{eff} , v_R and \bar{v}_R (or $\tan \delta$). The masses are close to these parameter values with corrections of few tens of GeV's.

The lightest chargino has a mass slightly below the soft gaugino masses and it is mostly a mixture of a bidoublet higgsino and a left-handed wino. One chargino is essentially a pure bidoublet higgsino with a mass $|\mu_{\text{eff}}|$. There is also a third sub-TeV chargino, which is also a combination of a bidoublet Higgsino and left-handed wino. The two heaviest charginos have masses of the order of v_R , i.e. they are in the multi-TeV region. These are mostly composed of the right-handed wino and the singly charged δ^{c-} ($\bar{\delta}^{c+}$).

The lightest chargino can always decay via $\tilde{\chi}_1^+ \rightarrow W^+ \tilde{\chi}_1^0$. The decay to $W^+ \tilde{\chi}_2^0$ is kinematically forbidden. In the case BP3 also $\tilde{\tau} \nu$ and $\tau \tilde{\nu}$ can be possible decay channels. Within the parameter regions the lighter stau could be lighter than the lightest neutralino. We discard such points.

The doubly charged higgsino has a mass $|\lambda v_s/\sqrt{2}|$, and therefore can be light and can have interesting collider signatures [28, 45, 59–63]. Since λ and v_s are in principle unconstrained, the mass of the doubly charged higgsino can vary over a wide region. Since we assume that the doubly charged Higgs coupling to taus is large to ensure large radiative corrections to the doubly charged Higgs mass and also its decay to $\tau^\pm \tau^\pm$ to dominate, the doubly charged higgsino will decay to $\tau^\pm \tilde{\tau}^\pm$ unless that mode is kinematically forbidden. If the stau is heavy, $\tilde{\chi}^{++} \rightarrow H_1^{++} \tilde{\chi}_1^0$ will be the dominant decay mode [64]. For our benchmarks $v_s \sim \text{TeV}$, and the doubly charged higgsinos are heavy.

3.2 Neutralinos

There are ten neutralinos in the spectrum. The neutralino mass matrix in the basis $(\tilde{\phi}_1, \tilde{\phi}_2, \tilde{\chi}_1, \tilde{\chi}_2, \tilde{\delta}^c, \tilde{\delta}^{\bar{c}}, \tilde{S}, \tilde{B}, \tilde{W}_L^0, \tilde{W}_R^0)$ is

$$M_{\tilde{\chi}^0} = \begin{pmatrix} 0 & 0 & 0 & -\mu_{eff} & 0 & 0 & -\mu_d & 0 & g_L v_u/\sqrt{2} & -g_R v_u/\sqrt{2} \\ 0 & 0 & -\mu_{eff} & 0 & 0 & 0 & 0 & 0 & 0 & 0 \\ 0 & -\mu_{eff} & 0 & 0 & 0 & 0 & 0 & 0 & 0 & 0 \\ -\mu_{eff} & 0 & 0 & 0 & 0 & 0 & -\mu_u & 0 & -g_L v_d/\sqrt{2} & g_R v_d/\sqrt{2} \\ 0 & 0 & 0 & 0 & 0 & \lambda v_s/\sqrt{2} & \lambda \bar{v}_R/\sqrt{2} & g' v_R & 0 & -g_R v_R \\ 0 & 0 & 0 & 0 & \lambda v_s/\sqrt{2} & 0 & \lambda v_R/\sqrt{2} & -g' \bar{v}_R & 0 & -g_R \bar{v}_R \\ -\mu_d & 0 & 0 & -\mu_u & \lambda \bar{v}_R/\sqrt{2} & \lambda v_R/\sqrt{2} & 0 & 0 & 0 & 0 \\ 0 & 0 & 0 & 0 & g' v_R & -g' \bar{v}_R & 0 & M_1 & 0 & 0 \\ g_L v_u/\sqrt{2} & 0 & 0 & -g_L v_d/\sqrt{2} & 0 & 0 & 0 & 0 & M_{2L} & 0 \\ -g_R v_u/\sqrt{2} & 0 & 0 & g_R v_d/\sqrt{2} & -g_R v_R & -g_R \bar{v}_R & 0 & 0 & 0 & M_{2R} \end{pmatrix}, \quad (3.2)$$

where $\mu_{u,d} = \lambda_{12} v_{u,d}/\sqrt{2}$.

With the superpotential and the parameter ranges used, the lightest neutralino is dominantly a singlino with a relatively large \tilde{W}_R^0 component. However the composition of the lightest neutralino depends crucially on the form of the superpotential. Terms of the form $M_S S^2$ and $\lambda_S S^3$ are gauge invariant and could be added to the superpotential if there are no additional symmetries that would forbid their existence. These terms contribute to the mass of the singlino-dominated state and may easily make it heavier than the lightest gaugino-dominated state.

The lightest gaugino-dominated state is mostly \tilde{W}_L^0 . Since the bino mixes with the neutral components of the fermionic triplets $\tilde{\Delta}^c$ and $\tilde{\bar{\Delta}}^c$, and the mixing terms $\tilde{B}\tilde{\Delta}^c$ and $\tilde{B}\tilde{\bar{\Delta}}^c$ are proportional to v_R and \bar{v}_R , respectively, even if the bino mass M_1 is the lightest gaugino mass, through mixing the bino dominated states will be heavier. If $|M_{2L}| < |\mu_{eff}|$, the \tilde{W}_L^0 is the second lightest neutralino (with mass slightly below $|M_{2L}|$), otherwise the bidoublet higgsino would be second lightest, with a mass $\sim |\mu_{eff}|$. For the case BP1 the average compositions of the lightest neutralinos and charginos are given in Table 4. The results for the BP3 case are essentially the same. The average masses and compositions (for BP2) of the lightest neutralinos and charginos are given in Table 5. With these parameters the charginos and neutralinos are lighter and the bidoublet states decouple and do not mix with the triplets or right-handed gaugino states as much as in BP1 or BP3 cases.

With our parameter choices for BP1 and BP3 benchmarks, the second lightest neutralino is more than 200 GeV heavier than the lightest one. This means that both of the channels $\tilde{\chi}_2^0 \rightarrow \tilde{\chi}_1^0 Z$ and $\tilde{\chi}_2^0 \rightarrow \tilde{\chi}_1^0 h$ are kinematically open. In the case of benchmark BP3 the channels $\tau\bar{\tau}$ and $\nu\bar{\nu}$ may be open if the stau or sneutrino are light enough. The \tilde{W}_L^0 -dominated state will dominantly decay to these channels if it is not the NLSP since the largest components in $\tilde{\chi}_1^0$ do not couple to W_L^0 . In the case BP2 both the lightest and the

Component	$\tilde{\chi}_1^0$	$\tilde{\chi}_2^0$	$\tilde{\chi}_3^0$	Component	$\tilde{\chi}_1^+$	$\tilde{\chi}_2^+$
$\tilde{\phi}_1$	0.84%	16.44%	—	$\tilde{\phi}^+$	—	71.98%
$\tilde{\phi}_2$	—	—	50.00%	$\tilde{\chi}^+$	52.04%	—
$\tilde{\chi}_1$	—	—	50.00%	$\tilde{\delta}^c +$	—	3.07%
$\tilde{\chi}_2$	0.29%	24.25%	—	\tilde{W}_L^+	47.96%	—
$\tilde{\delta}^c$	0.17%	—	—	\tilde{W}_R^+	—	24.96%
$\tilde{\tilde{\delta}}^c$	0.19%	—	—			
\tilde{S}	69.38%	0.09%	—			
\tilde{B}	0.06%	—	—			
\tilde{W}_L	0.09%	59.17%	—			
\tilde{W}_R	28.97%	0.03%	—			
Mass (GeV)	152.4	438.8	548.0		456.1	547.6

Table 4: The average masses and compositions of the lightest neutralinos and charginos for benchmark BP1. The values are almost the same for benchmark BP3.

Component	$\tilde{\chi}_1^0$	$\tilde{\chi}_2^0$	$\tilde{\chi}_3^0$	Component	$\tilde{\chi}_1^+$	$\tilde{\chi}_2^+$
$\tilde{\phi}_1$	0.60%	5.23%	—	$\tilde{\phi}^+$	—	99.83%
$\tilde{\phi}_2$	—	—	50.00%	$\tilde{\chi}^+$	54.91%	—
$\tilde{\chi}_1$	—	—	50.00%	$\tilde{\delta}^c +$	—	0.16%
$\tilde{\chi}_2$	1.42%	18.17%	—	\tilde{W}_L^+	45.09%	—
$\tilde{\delta}^c$	0.03%	—	—	\tilde{W}_R^+	—	0.01%
$\tilde{\tilde{\delta}}^c$	0.03%	—	—			
\tilde{S}	63.10%	0.24%	—			
\tilde{B}	0.07%	—	—			
\tilde{W}_L	0.58%	76.22%	—			
\tilde{W}_R	34.16%	0.13%	—			
Mass (GeV)	77.4	174.1	349.2		184.7	349.0

Table 5: The average masses and compositions of the lightest neutralinos and charginos for benchmark BP2.

second lightest neutralino masses are smaller than in the benchmarks BP1 or BP3. In this case the mass splitting is often around 100 GeV so that $\tilde{\chi}_2^0 \rightarrow \tilde{\chi}_1^0 h$ is not allowed on-shell. when that occurs, the dominant decays from NLSP to LSP would be the three-body decays $\tilde{\chi}_2^0 \rightarrow \tilde{\chi}_1^0 f \bar{f}$. The different neutralinos and charginos production in this model can give interesting signals at the LHC [65].

3.3 Sleptons

The slepton masses depend on the benchmark chosen. While the right-handed ones need to be heavier to generate a large doubly charged Higgs mass, the left-handed sleptons can be light in the BP3 scenario, as in Table 2. The sneutrino masses are largely determined by the soft slepton masses. For benchmarks BP1 and BP2 sneutrinos are heavy, whereas in

BP3 case the lightest sneutrino mass typically varies between (350 - 700) GeV. Hence for benchmark BP3 the left-handed sneutrino may be the second lightest neutral superpartner. If the sneutrino is the NLSP it will dominantly decays to $\nu_L \tilde{\chi}_1^0$, which is invisible.

4 The decay modes of H_1^0

In this section we discuss the light SM like Higgs boson, H_1^0 decays into the SM final states: $f\bar{f}, WW, ZZ, \gamma\gamma$ and gg , where last two decay modes are at one loop level. As evident from the discussion in Sec. 2, the observed scalar at the LHC would have to be a superposed state of the many physical scalar degrees of freedom in the LRSUSY Higgs sector. Thus the decay properties of such a Higgs with mass at ~ 125 GeV would crucially depend on its composition, which in turn would give us an insight on the parameter space of the model which allows the Higgs to behave as the one observed at the LHC. Note that the partial decay widths for channels which would be affected directly by new particles in the spectrum and that can couple to the Higgs boson are the loop induced decay modes, namely $H_1^0 \rightarrow g g, \gamma\gamma, Z\gamma$. The gg mode will be only affected through colored particles appearing in the loop. As current limits on the supersymmetric colored states from direct searches at the LHC are quite strong, they would be quite heavy and therefore should not affect the $H_1^0 \rightarrow g g$ partial width. This is also reflected in the parameter choice that we assume. However, the $\gamma\gamma, Z\gamma$ modes are definitely affected by the particles unique to the LRSUSY particle spectrum, such as the charged scalars (singly/doubly) and fermions and will play a major role. Note that a somewhat slight discrepancy in the Higgs observation is seen in the $\gamma\gamma$ mode, though reduced in the new CMS data [7], makes the aforementioned contributions in this model all the more worth considering.

4.1 $H_1^0 \rightarrow \gamma\gamma$

The $H_1^0 \rightarrow \gamma\gamma$ decay is a loop process involving the exchange of spin 0, 1/2, 1 particles in the loop. In our case, in addition to the SM contributions (mainly coming from top and W boson loop) we add contributions from charginos (lightest and second lightest states), both lighter and heavier staus, stops, sbottoms, singly and doubly charged Higgs bosons. The introduction of doubly charged Higgs boson is very crucial as this can lead to non-trivial contribution to this partial width simply because of its enhanced electromagnetic strength. The most general expression for $\Gamma(H \rightarrow \gamma\gamma)$ [66–68] in the presence of spin 0, 1/2 and 1 particles is given by:

$$\Gamma(H_1^0 \rightarrow \gamma\gamma) = \frac{\alpha^2 M_{H_1^0}^3}{1024\pi^3} \left| \sum_f \frac{2N_c Q_f^2}{m_f} g_{H_1^0 ff} A_{1/2}^h(\tau_f) + \frac{g_{H_1^0 VV}}{M_W^2} A_1^h(\tau_V) - \frac{N_{c,S} Q_S^2}{M_S^2} g_{H_1^0 SS} A_0^h(\tau_S) \right|^2 \quad (4.1)$$

where, f, V, S stands for fermions ($t, b, \tau, \tilde{\chi}_1^\pm, \tilde{\chi}_2^\pm$), vectors (W^\pm) and scalars ($H_1^\pm, H^{\pm\pm}, \tilde{t}_i, \tilde{b}_i, \tilde{\tau}_i, i = 1, 2$) respectively. Here $g_{H_1^0 ff}, g_{H_1^0 VV}$ and $g_{H_1^0 SS}$ represent the Higgs couplings with

fermions (f), SM gauge bosons (W^\pm) and with scalars (S) respectively, α is the fine-structure constant, $N_{c,S} = 3(1)$ for quarks, squarks (leptons, sleptons, singly and doubly charged scalars), $Q_{f,S}$ and m_f, M_S are the electric charge and mass of the fermions and scalars respectively in the loop. $\tau_i = M_{H_1^0}^2/4M_i^2$, where i represent fermion, vector and scalar particles as mentioned above.

The relevant loop functions are given by

$$A_0(\tau) = -[\tau - f(\tau)]\tau^{-2}, \quad (4.2)$$

$$A_{1/2}(\tau) = 2[\tau + (\tau - 1)f(\tau)]\tau^{-2}, \quad (4.3)$$

$$A_1(\tau) = -[2\tau^2 + 3\tau + 3(2\tau - 1)f(\tau)]\tau^{-2}, \quad (4.4)$$

and the function $f(\tau)$ is given by

$$f(\tau) = \begin{cases} [\sin^{-1}(\sqrt{\tau})]^2, & (\tau \leq 1) \\ -\frac{1}{4} \left[\log \left(\frac{1 + \sqrt{1 - \tau^{-1}}}{1 - \sqrt{1 - \tau^{-1}}} \right) - i\pi \right]^2, & (\tau > 1). \end{cases} \quad (4.5)$$

4.2 $H_1^0 \rightarrow Z\gamma$

Similarly the corresponding decay width of the Higgs (H_1^0) into $Z\gamma$ [69–72] also occurs at one loop level involving the exchange of spin 1/2, spin 1 and spin 0 particles in the loops:

$$\begin{aligned} \Gamma(H_1^0 \rightarrow Z\gamma) = & \frac{\alpha M_{H_1^0}^3}{512\pi^4} \left(1 - \frac{M_Z^2}{M_{H_1^0}^2} \right)^3 \left| \sum_f \frac{4N_c Q_f}{m_f} g_{Zf\bar{f}} g_{H_1^0 f \bar{f}} A_{1/2}^h(\tau_h^f, \tau_Z^f) \right. \\ & \left. + \frac{1}{2M_W^2} g_{H_1^0 VV} g_{ZVV} A_1^h(\tau_h^V, \tau_Z^V) + \frac{N_{c,S} Q_S}{M_S^2} g_{ZSS} g_{H_1^0 SS} A_0^h(\tau_h^S, \tau_Z^S) \right|^2, \end{aligned} \quad (4.6)$$

where the Higgs boson couplings to f, V, S are explained before. Here, $g_{Zf\bar{f}}, g_{ZWW}$ and g_{ZSS} represent Z boson couplings to f, W^\pm, S respectively. We define, $\tau_h^i = 4M_i^2/M_{H_1^0}^2, \tau_Z^i = 4M_i^2/M_Z^2$, where i represent fermion, vector and scalar particles as defined for $H_1^0 \rightarrow \gamma\gamma$ decay process. The corresponding loop-factors are given by

$$\begin{aligned} A_0^h(\tau_h, \tau_Z) &= I_1(\tau_h, \tau_Z), \\ A_{1/2}^h(\tau_h, \tau_Z) &= I_1(\tau_h, \tau_Z) - I_2(\tau_h, \tau_Z), \\ A_1^h(\tau_h, \tau_Z) &= 4(3 - \tan^2 \theta_W) I_2(\tau_h, \tau_Z) + [(1 + 2\tau_h^{-1}) \tan^2 \theta_W - (5 + 2\tau_h^{-1})] I_1(\tau_h, \tau_Z). \end{aligned} \quad (4.7)$$

The functions I_1 and I_2 are given by

$$\begin{aligned} I_1(\tau_h, \tau_Z) &= \frac{\tau_h \tau_Z}{2(\tau_h - \tau_Z)} + \frac{\tau_h^2 \tau_Z^2}{2(\tau_h - \tau_Z)^2} [f(\tau_h^{-1}) - f(\tau_Z^{-1})] \\ &\quad + \frac{\tau_h^2 \tau_Z}{(\tau_h - \tau_Z)^2} [g(\tau_h^{-1}) - g(\tau_Z^{-1})], \\ I_2(\tau_h, \tau_Z) &= -\frac{\tau_h \tau_Z}{2(\tau_h - \tau_Z)} [f(\tau_h^{-1}) - f(\tau_Z^{-1})], \end{aligned} \quad (4.8)$$

where the function $f(\tau)$ is defined in Eq. (4.5), and the function $g(\tau)$ is defined as

$$g(\tau) = \begin{cases} \sqrt{\tau^{-1} - 1} \sin^{-1}(\sqrt{\tau}), & (\tau < 1) \\ \frac{1}{2} \sqrt{1 - \tau^{-1}} \left[\log \left(\frac{1 + \sqrt{1 - \tau^{-1}}}{1 - \sqrt{1 - \tau^{-1}}} \right) - i\pi \right], & (\tau \geq 1). \end{cases} \quad (4.9)$$

4.3 $H_1^0 \rightarrow XX$

The partial widths of the decay modes which proceed via tree level sub-processes will also vary and mostly depend on the choice of the different parameters of the LRSUSY model which govern the composition of the ~ 125 GeV scalar boson as discussed in Sec. 2. This in turn would modify its coupling to the fermions and weak gauge bosons and affect its respective partial decay widths.

The superpotential has a term of the form $Y_u Q_L \Phi_1 Q_R$. Hence the coupling of ϕ_2^0 to b -quarks is proportional to the top Yukawa coupling. Whenever the SM-like Higgs has a sizable ϕ_2^0 -component the Higgs coupling to b -quarks is altered significantly. Depending on the relative sign between the components in the eigenvector, the coupling may either increase significantly or become close to zero (or change sign).

At tree-level the mixing between $\{\phi_1, \chi_2\}$ and $\{\phi_2, \chi_1\}$ is zero [47]. Hence the admixture of ϕ_2^0 in the SM-like Higgs boson comes entirely from loop corrections. The dominant contribution comes from third generation quark and squark loops. The contribution of these diagrams is proportional to the product of top and bottom Yukawa couplings. This product, and hence the mixing element, is large at large values of $\tan\beta$. The mixing effect is significant when the second lightest Higgs is non-decoupled, which happens at values of $\tan\delta$ close to one.

Since $h \rightarrow b\bar{b}$ is the dominant decay mode, a substantial change in this coupling will change all other branching ratios. Hence there is an anti-correlation between the $h \rightarrow b\bar{b}$ signal strength and all other signal strengths. The effect is so strong that it leads to a strong correlation between all other signal strengths. We highlight this behavior in the next section when we discuss the fit to the Higgs data from our parameter scans. The corresponding correction for the Higgs- $\tau\tau$ coupling is proportional to the neutrino Yukawa coupling and is hence smaller. Thus the Higgs- $\tau\tau$ coupling is close to the Standard Model prediction. Since $\langle\phi_2^0\rangle = 0$, there is no three-point coupling for ϕ_2 and vector bosons, and when the SM-like Higgs has a sizable ϕ_2 -component, the couplings to vector bosons will be suppressed.

5 Implications for model parameters

The detailed discussion on the left-right supersymmetric spectrum in Sec. 3 gives us an idea of the parameters that could directly play a significant role in Higgs physics. Therefore we set a number of free parameters to fixed values as shown in Table 1 and perform random scans over the ranges of the input parameters shown in Table 2. We divide the choice for fixed values and the corresponding scans into three benchmark points while we have ensured that the current limits on supersymmetric particles are respected through all the scans. We

also make sure that one of the Higgs mass is always within $122 \text{ GeV} < M_h < 128 \text{ GeV}$ and compare its properties to the scalar resonance that has been observed at the LHC.

As the LHC experiments have not observed any signal indicative of beyond the SM physics, the most stringently constrained sector in almost all extensions of SM is the strongly interacting sector. Therefore we cannot choose very light squark and gluino masses which would be ruled out by experimental data. Note that we have chosen our parameter space as shown in Tables 1 and 2 where the gluino mass as well as the squark masses are around $\sim 1 \text{ TeV}$. A large mixing in the third generation is however still allowed to give a significant splitting for the stop mass eigenstates. In addition, the $SU(2)_R$ breaking scale is also strongly constrained from direct searches for right-handed gauge bosons (W_R, Z_R). We have therefore chosen v_R to be sufficiently large to evade the existing mass bounds on such gauge bosons at the LHC. For the remaining parameters we make sure that our model spectrum is consistent with these experimental constraints [73] :

- Lower limits on superpartner masses from LEP and the 7 & 8 TeV run of the LHC.
- Low energy flavour physics processes : $b \rightarrow s\gamma$, $B_s \rightarrow \mu^+\mu^-$.

The superpartner masses are controlled by the choices of soft mass parameters and the μ -parameter. We also require the lightest neutralino to be heavier than $m_h/2$ so that invisible Higgs decays are kinematically forbidden.

The flavour constraints are taken care of by requiring $m_A > 300 \text{ GeV}$ and limiting $\tan\beta$ from above. The lightest charged Higgs contributes to $b \rightarrow s\gamma$ but in supersymmetric models the contribution from the chargino cancels partially that of the charged Higgs. The mass of the charged Higgs follows closely the lightest CP-odd Higgs mass as can be seen from Fig. 2. The reaction $B_s \rightarrow \mu\mu$ is mediated by the lightest CP-odd Higgs. That contribution is at largest at large values of $\tan\beta$. On the other hand, as discussed previously, the Higgs coupling to b-quarks is often altered at large $\tan\beta$ so much that it would be experimentally excluded.

We analyze numerically the various Higgs decay modes in our model and study to what extent they differ from the SM predictions. The enhancement or the suppression over the SM can be studied using the signal strengths (R_{XX}), defined as the Higgs production cross section times the branching ratio, normalized to the SM value:

$$R_{XX} = \frac{\sigma(pp \rightarrow h) \times BR(h \rightarrow XX)}{\sigma(pp \rightarrow h)_{SM} \times BR(h \rightarrow XX)_{SM}} \quad (5.1)$$

Here $\sigma(pp \rightarrow h)$ gives the on-shell production cross-section of the Higgs boson. For the Higgs production modes, we have considered gluon-gluon fusion (gg) and the associated vector boson production (VH), where V stands for W or Z boson. While for most of the decay channels, gg production mode is considered, we use the VH mode for $b\bar{b}$ and $\tau^+\tau^-$ final states.

The Higgs production cross-section through gg fusion is calculated both in the LRSUSY and in the SM, using the publicly available package HIGLU [74], at LHC with the center of mass energy, $\sqrt{s} = 8 \text{ TeV}$. As the cross section for the Higgs production implemented in

HIGLU is for the SM, we calculated the effective coupling strengths in the LRSUSY model and obtained the cross sections by modifying the strengths in the HIGLU code. The partial decay widths evaluation for the Higgs is done using another publicly available package HDECAY [75]. A similar technique to what was done in HIGLU is used here too to get the partial widths in the LRSUSY model. However, the loop induced decay modes, $h \rightarrow \gamma\gamma$ and $h \rightarrow Z\gamma$ involve new particles modifying the loop amplitudes, and here we used our Fortran code. Note that HIGLU includes the QCD correction while calculating the Higgs production cross-section. Any explicit implementation of QCD or EW corrections are not taken into account in calculating the partial decay widths of $H_1^0 \rightarrow \gamma\gamma$ or $H_1^0 \rightarrow Z\gamma$ modes. However, we expect that the EW contribution to these decays will be the same as in the SM and thus cancel out when we consider the signal strengths.

Higgs decay channel	Experiment	\sqrt{s} (TeV) (Luminosity in fb^{-1})	Signal strengths
$h \rightarrow \tau\bar{\tau}$	ATLAS	8(20.3)	$1.4^{+0.5}_{-0.4}$
$h \rightarrow \tau\bar{\tau}$	CMS	7(5.1) + 8(19.7)	$0.91^{+0.27}_{-0.27}$
$h \rightarrow b\bar{b}$	ATLAS(VH)	7(4.7) + 8(20.3)	$0.2^{+0.7}_{-0.6}$
$h \rightarrow b\bar{b}$	CMS(VH)	7(5.1) + 8(18.9)	$0.93^{+0.49}_{-0.49}$
$h \rightarrow WW^*$	ATLAS	7(4.6) + 8(20.7)	$1.00^{+0.32}_{-0.29}$
$h \rightarrow WW^*$	CMS	7(5.1) + 8(19.7)	$0.83^{+0.21}_{-0.21}$
$h \rightarrow ZZ^*$	ATLAS	7(4.6) + 8(20.7)	$1.44^{+0.40}_{-0.35}$
$h \rightarrow ZZ^*$	CMS	7(5.1) + 8(19.7)	$1.00^{+0.29}_{-0.29}$
$h \rightarrow \gamma\gamma$	ATLAS	7(4.8) + 8(20.7)	$1.57^{+0.33}_{-0.29}$
$h \rightarrow \gamma\gamma$	CMS	7(5.1) + 8(19.6)	$1.13^{+0.24}_{-0.24}$

Table 6: The measured values for the Higgs signal strength, and their corresponding uncertainties (lower/upper edges of 1σ error bars), in the various channels [5–7].

We list the observed strengths for the Higgs signal in different final state modes by the ATLAS [5] and CMS [6, 7] experiments in Table 6. It is worth mentioning here that we found that there exists enough model (LRSUSY) parameter space within the 2σ limit of the ATLAS and CMS results of Higgs signal strengths. To illustrate our findings, we can choose either the CMS or the ATLAS results. The generic features of the fit would remain very similar and a definite shift is found in the allowed parameter space when using the ATLAS data as the central values and the associated errors for the different channels in the two experiments do allow for a wide range of signal strength values. However there is a definite overlapping region of the parameter space which is common and satisfies data from both experiments. As an extension of our findings and for better understanding of the model, we first study the variations of few of the relevant sparticle masses with $\tan\beta$, for which the signal strengths R_{WW^*} and $R_{\gamma\gamma}$ are simultaneously within the 2σ error bar of CMS result (see Table. 6). We do this for all the three benchmark points to study the parameters that would affect the signal strengths in a significant way.

We choose the R_{WW^*} and $R_{\gamma\gamma}$ results, since these provide the most stringent bound on the parameter space. In Fig. 3(a), we show the allowed values for the mass of the doubly

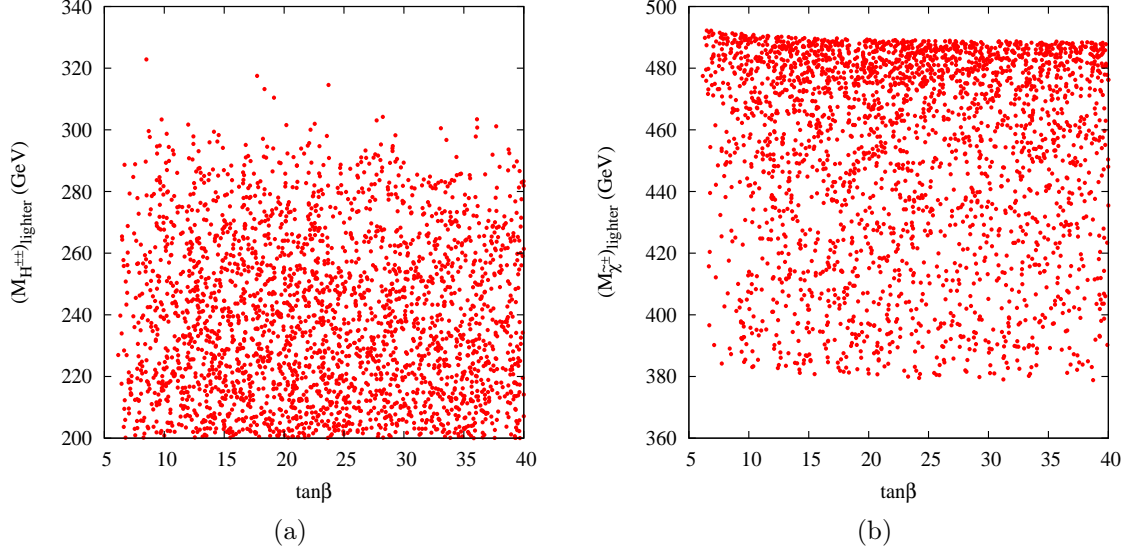


Figure 3: Allowed parameter space for benchmark BP3 in the (a) $\tan\beta - M_{H^{\pm\pm}}$ and (b) $\tan\beta - M_{\tilde{\chi}^{\pm\pm}}$ plane, where $R_{\gamma\gamma}$ and R_{WW^*} are within 2σ of CMS result.

charged Higgs mass ($M_{H^{\pm\pm}}$) as a function of $\tan\beta$ for the BP3 scenario. Note that the variation in $\tan\beta$ does not play any significant role for the doubly charged scalar mass, but does affect the signal strength for the 125 GeV Higgs in the fermionic decay modes. This in turn would affect the branching in the $\gamma\gamma$ mode where the light doubly charged scalar contributes in the loop. The Higgs mass and the resulting bound on $\tan\beta$ have an effect on the coupling between the SM-like Higgs and the doubly charged Higgs bosons, which can be seen as follows. If we write the lighter doubly charged Higgs state as $H_1^{++} \equiv a \delta^{c++} + b \bar{\delta}^{c++}$, the coupling between the SM-like Higgs and the doubly charged Higgs is

$$g_{hH^{++}H^{--}} = -\sqrt{2}ab \frac{\lambda v \mu_{\text{eff}}}{v_s} \sin 2\beta + \frac{1}{4}(a^2 - b^2)g_R^2 v. \quad (5.2)$$

The lighter state is almost the symmetric combination with values around $a = 0.73$ and $b = 0.69$. Hence the term $a^2 - b^2$ is quite small. At large or even moderate values of $\tan\beta$, the value of $\sin 2\beta$ is small so the coupling will be quite limited. This leads to an interesting observation in the LRSUSY model. We find here that the doubly charged scalar contribution is therefore comparatively less than that of the singly charged scalars in both $H \rightarrow \gamma\gamma$ and $H \rightarrow Z\gamma$ processes, simply because the $h - H^{\pm\pm} - H^{\mp\mp}$ coupling is weaker than $h - H^{\pm} - H^{\mp}$ coupling. A relative suppression at the level of relative coupling strength is found to be $g_{hH^{\pm\pm}H^{\mp\mp}}/g_{hH^{\pm}H^{\mp}} \approx 1/20$ and this makes the doubly charged contribution substantially smaller than singly charged one. This behavior is completely opposite to Type-II Seesaw models [76–78], where the largest contribution to these one-loop processes comes from the virtual exchange of doubly charged scalars.

Due to the form of the tree-level bound it is very difficult to have a Higgs mass around 125 GeV when $\tan\beta$ is close to 1, where the coupling between the Higgs and doubly charged Higgs bosons would be large. Therefore an indirect dependence on its mass can be obtained as a function of $\tan\beta$ here. As discussed in Sec. 3, a large value of the soft parameter $(M_{\tilde{\ell}})_R$ helps in raising the doubly charged Higgs mass through radiative corrections, to above its current experimental limits of 200 GeV, provided it decays with 100% probability into $\tau^\pm\tau^\pm$. We also note that the upper limit of the range over which this parameter is scanned for benchmark BP3 is much lower than that for the other two benchmark points. Thus we find that much lighter doubly charged scalars are preferred and also satisfy the CMS data. Very similar feature is observed for BP1 and BP2 cases, but as the scan range over $(M_{\tilde{\ell}})_R$ is for larger values, we also get heavier doubly charged states in the spectrum for these benchmark points. In Fig. 3(b) we show the lightest chargino mass as a function of $\tan\beta$. In this case, there is a dependence on $\tan\beta$ as seen from Eq. 3.1. However the dominant parameter is the value for parameters M_2 and μ_{eff} which set the upper limit of the lighter chargino mass to ~ 200 GeV for BP2 and ~ 500 GeV for BP1 and BP3 scenarios respectively, and we observe that the bounds from Higgs signal strengths allow almost all the available mass region. This is illustrated for BP3 case in Fig. 3 (b). In Fig. 4 we

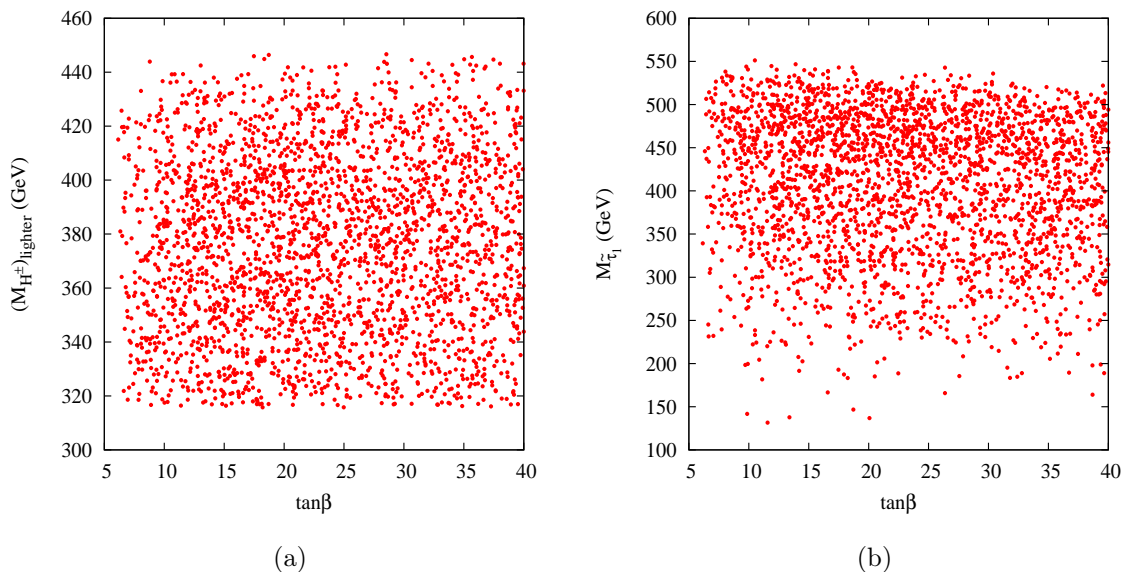


Figure 4: Allowed parameter space for BP3 scenario in the (a) $\tan\beta - M_{H^\pm}$ and (b) $\tan\beta - M_{\tilde{\tau}_1}$ plane, where $R_{\gamma\gamma}$ and R_{WW^*} are within 2σ of CMS result.

show the variation of lighter singly charged Higgs boson mass with $\tan\beta$ as well as the lightest stau ($\tilde{\tau}_1$) mass for the benchmark point BP3. It is important to note that, while for BP1 and BP2 cases, the lighter singly charged Higgs mass can vary from 300 GeV to 650 GeV, it is in the range 320-450 GeV for BP3 scenario. As discussed before, and also seen in Fig. 2, a large $\tan\delta$ value yields a lighter singly charged scalar in the spectrum.

This is the case in BP3 where the scan runs over larger values of $\tan\delta$. We checked for the consistency of such light charged scalars with flavour physics constraints and we find that the Higgs data gives a much weaker constraint compared to flavour physics limits, which we include. We also find that a much lighter $\tilde{\tau}_1$ is allowed, consistent with our choice of parameters for benchmark BP3, and the Higgs data does not constrain them very much either. Note that $\tilde{\tau}_1$ is significantly heavier for the other benchmark BP1 and BP2 due to the parameter choice for the scan of the slepton soft mass parameters. Thus we find that a large region of the parameter space in the left-right supersymmetric scenario still survives when

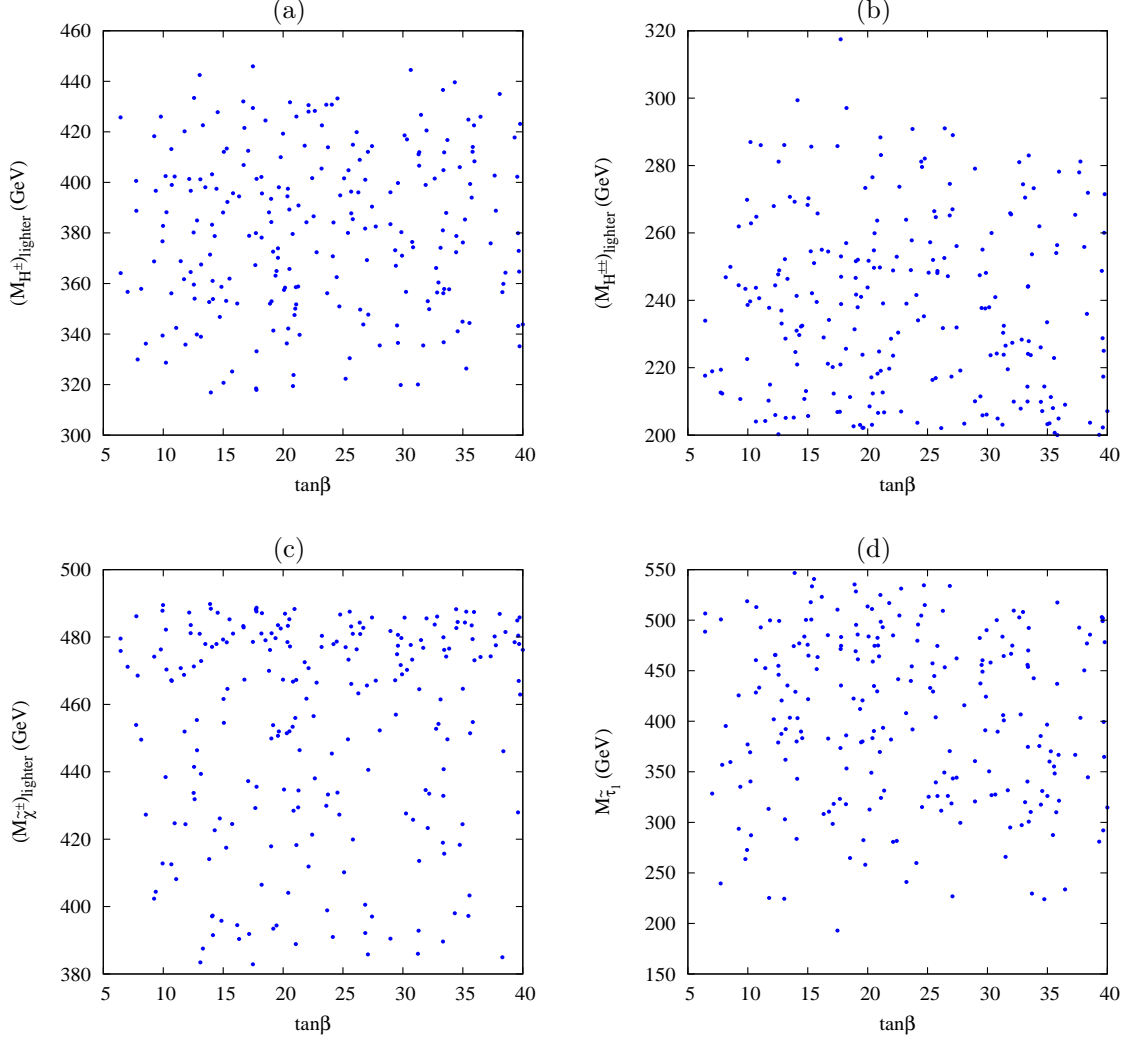


Figure 5: Allowed parameter space for benchmark point BP3 in the plane $\tan\beta$ and (a) M_{H^\pm} (b) $M_{H^{\pm\pm}}$, (c) $M_{\tilde{\chi}^\pm}$, (d) $\tan\beta - M_{\tilde{\tau}_1}$, where $R_{\gamma\gamma}$ and R_{WW^*} are within 2σ of CMS result and the points indicate those values for which the lightest CP-even Higgs coupling is within 2% of SM value.

confronted by the Higgs data at LHC. Light singly- and doubly-charged scalars, sleptons (benchmark BP3) and charginos (benchmark BP2) are all viable and agree with the Higgs

signal strengths. Of course when one considers the parameter scan, it is also imperative to view the scan where the SM coupling strengths are not altered by large values. There can be two ways of achieving this. The most likely case would be the case where the SM sector is completely decoupled and none of the supersymmetric particles contribute to the Higgs decay. The other and more interesting option would be to consider the non-decoupling scenario, where the supersymmetric particles conspire in their contributions to give similar coupling strengths as the SM Higgs. This would mean that a light left-right supersymmetric spectrum would still coexist and is waiting to be discovered at the LHC.

It is therefore interesting to check the presence of the LRSUSY model even if the Higgs coupling is almost SM like. Therefore, for illustration purposes, we set the lightest CP-even Higgs couplings to all SM particles within 2% of the SM value and calculate the Higgs signal strengths³. We analyze this by studying the allowed parameter space only for benchmark point BP3. A few things worth noting here is that although the $ht\bar{t}$ and hWW couplings are not affected at all throughout the scan, the $hb\bar{b}$ is affected significantly, as discussed earlier. So we find this to be the dominating factor in allowing only a 2% shift. As can be seen from Fig. 5, there still exists a strong possibility of having a light LRSUSY spectrum, even if the Higgs couplings are very close to the SM values. The blue points in Fig. 5 show that quite a significant parameter range of LRSUSY which is light and can modify the Higgs decays to conspire and give SM like strength for the ~ 125 GeV scalar state for the observed decay modes. Or it is equally possible to have these light states which do not shift the Higgs couplings by large amounts but will show up in other complementary channels through direct production at the LHC running with high enough luminosity.

We now focus on the signal strengths that we obtain through our scan over the different parameters in the LRSUSY model. Figs. 6 and 7 show the correlations among the various signal strengths. The scanned parameter points in the LRSUSY model are shown in red. The black solid triangle represents the best-fit point of the ATLAS Collaboration, with the patterned blue and magenta patches showing regions of 1σ and 2σ uncertainty respectively, while the black circle denotes the best-fit value of the signal rates predicted by the CMS Collaboration with the solid green and yellow patches show the 1σ and 2σ uncertainty around it, respectively. In Table. 6, we give the experimental values of the signal rates for different Higgs decay channels with the corresponding center of mass energy and integrated luminosity. When compared to the mass plots which only use the CMS data, we do find that there exists a much extended parameter space for the LRSUSY model which is allowed by current Higgs data. The ATLAS results in fact give a much larger acceptance for the parameter space when compared to the CMS. We find regions where the couplings are consistent with the SM values as well as regions where they can significantly vary and modify the signal strengths beyond the SM expectations. Note that both R_{WW} and R_{ZZ} are almost linearly correlated to $R_{\gamma\gamma}$. However that is not the case when one considers the R_{bb} shown in Fig. 7. We find that R_{bb} is anti-correlated to all the other signal rates, as also evident from Fig. 7. This is simply because the Higgs boson decays mostly into $b\bar{b}$ final

³We should however point out that such a high precision for the measurement of all the Higgs couplings would be extremely difficult at the LHC even at very high luminosity.

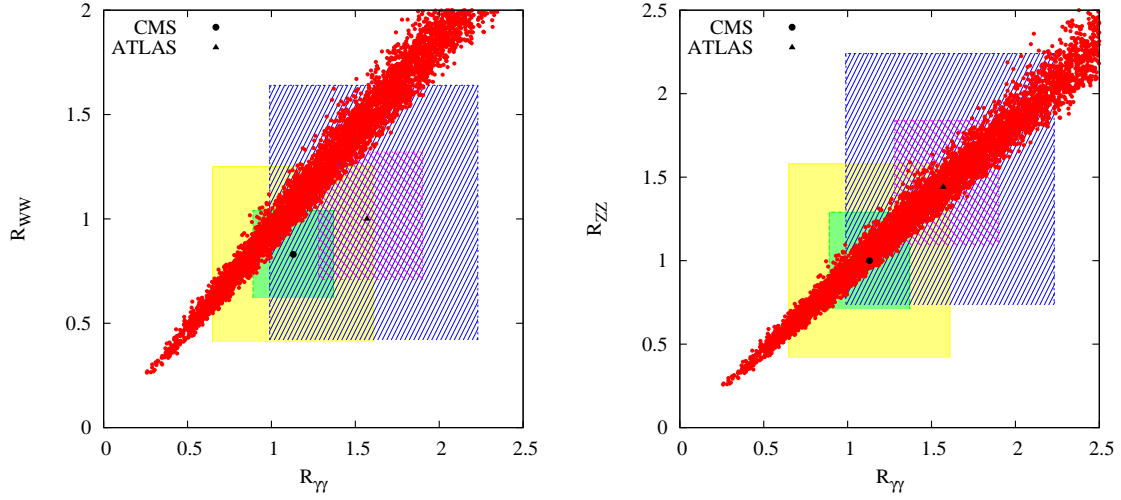


Figure 6: Correlation between signal strengths for the Higgs boson in the $\gamma\gamma - WW^*$ (left panel) and $\gamma\gamma - ZZ^*$ (right panel) channel in the LRSUSY model for the benchmark BP3. The corresponding central values as observed by the CMS (circular black point) and ATLAS (triangular black point) Collaborations in the two channels are shown. We also include the associated 1σ and 2σ deviations allowed by the data, shown as overlying rectangles around the central values. For details see the text.

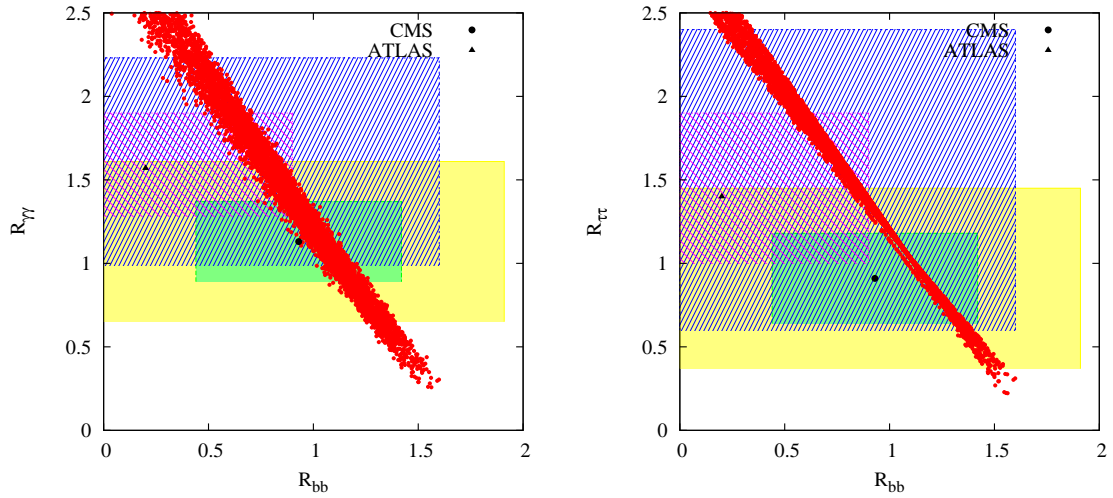


Figure 7: Correlation between signal strengths for the Higgs boson in the $b\bar{b}$, $\gamma\gamma$ and $\tau\bar{\tau}$ channel in the LRSUSY model for benchmark BP3. Color specifications are same as Fig. [6].

states and hence the total decay width is dependent sensitively on the partial decay width $\Gamma(H \rightarrow b\bar{b})$. Hence, an increase in $b\bar{b}$ branching ratio will effectively reduce the branching ratios of sub-dominant decay channels. All the other rates show strong correlations among each other. Hence, we see that our model provides a large parameter space greatly consistent with the present LHC data. With the LHC expected to run with greater energy and gather

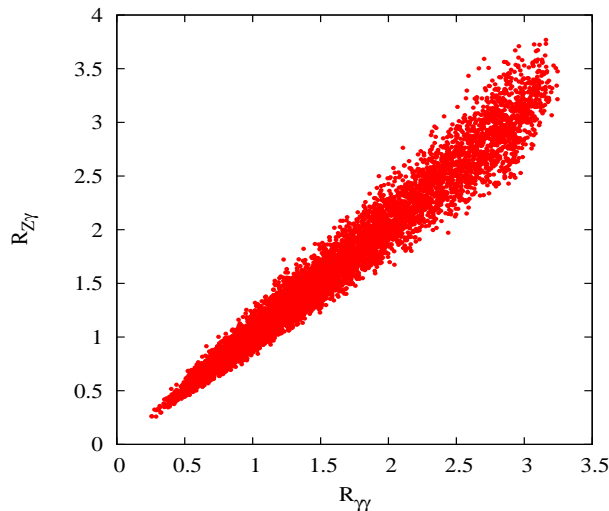


Figure 8: Predicted correlation between signal strengths for the Higgs in the $\gamma\gamma$ and $Z\gamma$ channel in the LRSUSY model for the benchmark BP3 at the LHC with center of mass energy of 14 TeV.

data with higher integrated luminosity, it is quite clear that it will also be able to measure the Higgs signal in other channels which it could not at the $\sqrt{s} = 7$ and 8 TeV. One such mode would be the remaining loop mediated decay channel $Z\gamma$. As the LRSUSY model also affects that mode, similar to the $\gamma\gamma$, we present the expected correlation between the signal strengths of the Higgs in the two modes $R_{\gamma\gamma}$ and $R_{Z\gamma}$ at the 14 TeV run of LHC in Fig. 8 for the benchmark point BP3.

At the next run, LHC at 14 TeV with 300 fb^{-1} luminosity, the decay $H \rightarrow \gamma\gamma$ is expected to be measured with an accuracy of 10% [79, 80]. With such precision, our restrictions for the parameter space of the LRSUSY model will tighten considerably. In anticipation, we illustrate in Fig. 9 for BP3 the range of low lying LRSUSY weakly (left panel) and strongly (right panel) interacting masses as a function of $\tan\beta$ imposing the signal strengths $\mu(gg \rightarrow H \rightarrow \gamma\gamma)$ to be measured with a precision of 10%. Among weakly interacting particles (charged Higgs bosons, charginos and staus), besides the LSP, the lowest lying particle is the doubly charged scalar, whose mass can be as light as (200-300) GeV, while the heaviest one is the $\tilde{\tau}_2$ with the mass in the range (450-600) GeV. All these particles will be easily accessible at the early run of the 14 TeV LHC. On the other hand most of the strongly interacting particles (stop and sbottom) are heavier, falling in the

(1-1.4) TeV mass range. From these two figures, it clear that the mass spectrum is almost independent of variations in $\tan\beta$. Note that we did not use measurements on other Higgs signal channels as they have uncertainties larger than 20%.

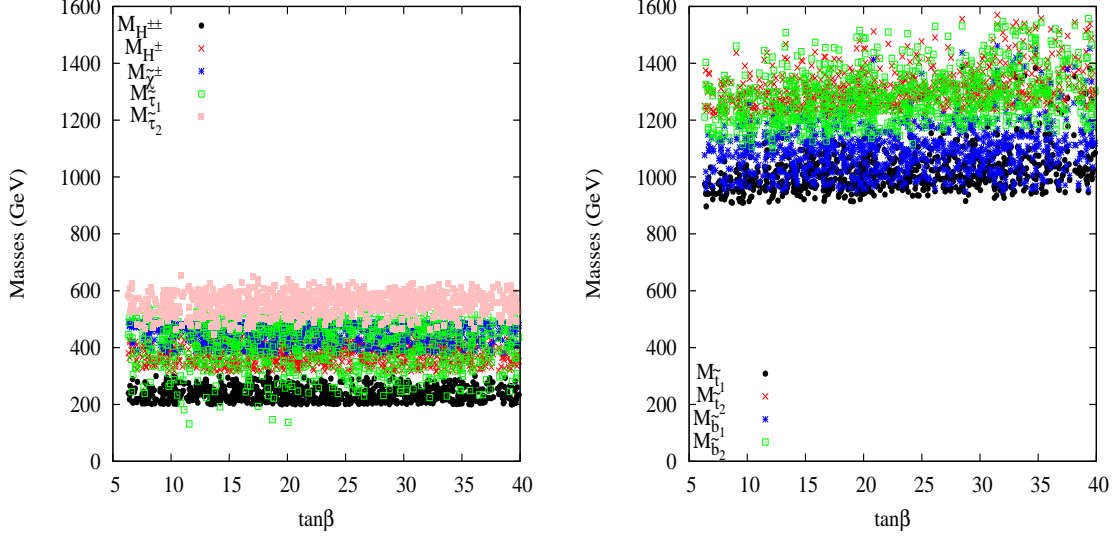


Figure 9: The low lying mass spectrum of LRSUSY model as a function of $\tan\beta$ for $\mu(gg \rightarrow H, H \rightarrow \gamma\gamma) = 1 \pm 0.1$ at 14 TeV LHC with 300 fb^{-1} luminosity. The left and right panels show weakly and strongly interacting particle masses, respectively.

6 Conclusions

In this paper we studied the implications of different Higgs signal strengths as measured at the LHC on the parameter space of the left-right supersymmetric model (LRSUSY), especially on the Higgs, chargino and neutralino and scalar lepton sector. The LRSUSY models are based on by enlarging the standard model (SM) gauge group to $SU(3)_C \otimes SU(2)_L \otimes SU(2)_R \otimes U(1)_{B-L}$. The gauge structure and particle contents of this model are such that it can generate the tiny masses for neutrinos as well as solve the strong and the EW CP problems. This model predicts a plethora of new particles, among them the most important ones are singly and doubly charged Higgs bosons and higgsinos, which play crucial role in the one-loop mediated Higgs boson decay in $\gamma\gamma$ and $Z\gamma$ channels. We presented a complete description of this model and chose certain benchmark points by fixing some basic parameters of the model, while scanning over some other relevant parameters for the study of the Higgs bosons decay patterns. It turns out that the lightest Higgs boson, whose mass is close to 125 GeV and the lighter charged scalars are mostly components of the Higgs $SU(2)$ bidoublet, while the right handed $SU(2)$ triplet yields the doubly charged scalar. In our analysis we assumed that the decay $H^{++} \rightarrow \tau^+\tau^+$ dominates, while other

decay modes are negligible, and this allowed us to adopt the lower limit of 200 GeV for the doubly charged Higgs boson masses, in agreement with limits obtained at the LHC.

We estimated several Higgs signal strengths, defined as R_{XX} , in this model. For these, we selected a particular benchmark point, namely the BP3 and commented on changes expected by adopting BP1 or BP2 benchmarks. For the BP3 benchmark, we calculated explicitly the R_{XX} values and then compared with the experimental values quoted by both ATLAS and CMS for $\sqrt{s} = 7$ TeV and 8 TeV at 2σ precision. We found that sufficient LRSUSY model parameter space survives within the 2σ limit. To illustrate our findings, we considered either CMS or ATLAS results. Among the different channels, we emphasized mainly R_{WW^*} and $R_{\gamma\gamma}$ results, as these two are the most accurate and thus provide the most stringent limits on the parameter space.

In this scenario the one-loop mediated process, like $H \rightarrow \gamma\gamma$ and $H \rightarrow Z\gamma$, receive new contributions from doubly charged scalars and doubly charged higgsinos in addition to other supersymmetric particles. It is interesting to note that here the doubly charged scalar contribution is less than that of the singly charged scalars in both $H \rightarrow \gamma\gamma$ and $H \rightarrow Z\gamma$ processes, simply because the $h - H^{\pm\pm} - H^{\mp\mp}$ coupling is weaker than $h - H^{\pm} - H^{\mp}$ coupling, with a relative suppression of $\approx 1/20$ which makes the doubly charged contribution substantially smaller than singly charged one. This behavior is completely opposite to Type-II Seesaw models, where the largest contribution to these one-loop processes come from the virtual exchange of doubly charged scalars. Hence, perhaps this feature can be used to distinguish this model from other models which also include doubly charged scalars.

We also showed correlations (anti-correlations) among different R_{XX} values of the Higgs signal strengths by taking into account both the ATLAS and CMS experimental results at 1σ and 2σ level. In particular, we found a nice correlation between R_{VV^*} and $R_{\gamma\gamma}$, with $V = W^{\pm}, Z$. Our model predictions for these Higgs signal strengths in the BP3 benchmark showed good agreement with both the ATLAS and CMS at 2σ level, each of which could be matched individually, but not simultaneously, at 1σ level. This effect can be understood from the large difference between the experimental central values and the corresponding error bars.

The Higgs boson total width comes mainly from the Higgs partial decay width into $b\bar{b}$ final states, as expected, and this decay width is responsible in controlling patterns of $R_{\gamma\gamma}$. We have showed that there is clear anti-correlation between $R_{\gamma\gamma}$ and R_{bb} as well as between $R_{\tau\tau}$ and R_{bb} . This is explained from the fact that any increase in the partial width of $H \rightarrow b\bar{b}$ would lead to a suppression in the partial widths of the Higgs boson into other channels, namely into $\gamma\gamma$ and $\tau^+\tau^-$ final states. Once again for benchmark BP3, we showed that clear overlap regions are allowed at 2σ level from both the ATLAS and CMS experimental data on $R_{\gamma\gamma}, R_{bb}$ and $R_{\tau\tau}$.

Assuming the fixed parameters from Table 1 for BP3, we finally predicted the low lying weakly and strongly interacting mass spectrum for the LRSUSY model if the decay width $H \rightarrow \gamma\gamma$ would be measured at the level of 10% at 14 TeV LHC run with 300 fb^{-1} luminosity, as it is expected. We hope that some of these low lying particles will be seen and explored at the early run of the 14 TeV LHC.

Acknowledgments

D.K.G. and I.S. would like to acknowledge the hospitality provided by the High Energy Division, the Abdus Salam International Centre for Theoretical Physics (ICTP) and RECAPP, HRI where part of this work was done. The work of S.K.R. was partially supported by funding available from the Department of Atomic Energy, Government of India, for the Regional Centre for Accelerator-based Particle Physics (RECAPP), Harish-Chandra Research Institute (HRI). D.K.G. and S.K.R. would also like to thank the University of Helsinki and the Helsinki Institute of Physics, where this work was started and a major part of it was done and written. M.F. thanks the groups at HRI, IACS, India, and the University of Helsinki and the Helsinki Institute of Physics, and NSERC for partial financial support under grant number SAP105354. K.H. and H.W. acknowledge support from the Academy of Finland (Project No. 137960).

References

- [1] S. Chatrchyan *et al.* [CMS Collaboration], Phys. Lett. B **716** (2012) 30 [arXiv:1207.7235 [hep-ex]].
- [2] G. Aad *et al.* [ATLAS Collaboration], Phys. Lett. B **716** (2012) 1 [arXiv:1207.7214 [hep-ex]].
- [3] G. Aad *et al.* (ATLAS Collaboration), Phys. Rev. Lett. **108** (2012) 111803, arXiv:1202.1414 [hep-ex].
- [4] S. Chatrchyan *et al.* (CMS Collaboration), Phys. Lett. B **710** (2012) 403, arXiv:1202.1487 [hep-ex].
- [5] [ATLAS Collaboration], ATLAS-CONF-2014-009.
- [6] [CMS Collaboration], CMS-PAS-HIG-14-009.
- [7] V. Khachatryan *et al.* [CMS Collaboration], arXiv:1407.0558 [hep-ex].
- [8] H. Flacher, M. Goebel, J. Haller, A. Hocker, K. Monig and J. Stelzer, Eur. Phys. J. C **60**, 543 (2009) [Erratum-ibid. C **71**, 1718 (2011)] [arXiv:0811.0009 [hep-ph]].
- [9] M. Baak and R. Kogler, arXiv:1306.0571 [hep-ph].
- [10] P. P. Giardinio, K. Kannike, I. Masina, M. Raidal and A. Strumia, JHEP **1405**, 046 (2014) [arXiv:1303.3570 [hep-ph]].
- [11] G. Belanger, B. Dumont, U. Ellwanger, J. F. Gunion and S. Kraml, Phys. Rev. D **88**, 075008 (2013) [arXiv:1306.2941 [hep-ph]].
- [12] A. Arhrib, R. Benbrik and N. Gaur, Phys. Rev. D **85** (2012) 095021 [arXiv:1201.2644 [hep-ph]].
- [13] B. Swiezewska and M. Krawczyk, Phys. Rev. D **88** (2013) 3, 035019 [arXiv:1212.4100 [hep-ph]].
- [14] P. Draper and D. McKeen, Phys. Rev. D **85** (2012) 115023 [arXiv:1204.1061 [hep-ph]].
- [15] F. Arbabifar, S. Bahrami and M. Frank, Phys. Rev. D **87**, 015020 (2013) [arXiv:1211.6797 [hep-ph]].
- [16] A. G. Akeroyd and S. Moretti, Phys. Rev. D **86** (2012) 035015 [arXiv:1206.0535 [hep-ph]].

- [17] I. Picek and B. Radovic, Phys. Lett. B **719** (2013) 404 [arXiv:1210.6449 [hep-ph]].
- [18] L. G. Almeida, E. Bertuzzo, P. A. N. Machado and R. Z. Funchal, JHEP **1211** (2012) 085 [arXiv:1207.5254 [hep-ph]].
- [19] C. -W. Chiang and K. Yagyu, Phys. Rev. D **87** (2013) 3, 033003 [arXiv:1207.1065 [hep-ph]].
- [20] M. Carena, I. Low and C. E. M. Wagner, JHEP **1208** (2012) 060 [arXiv:1206.1082 [hep-ph]].
- [21] P. Bandyopadhyay, S. Di Chiara, K. Huitu and A. S. Keceli, arXiv:1407.4836 [hep-ph].
- [22] A. Delgado, G. Nardini and M. Quiros, Phys. Rev. D **86** (2012) 115010 [arXiv:1207.6596 [hep-ph]].
- [23] T. Kitahara, JHEP **1211** (2012) 021 [arXiv:1208.4792 [hep-ph]].
- [24] L. Basso and F. Staub, Phys. Rev. D **87** (2013) 015011 [arXiv:1210.7946 [hep-ph]].
- [25] T. Flacke, K. Kong and S. C. Park, Phys. Lett. B **728**, 262 (2014) [arXiv:1309.7077 [hep-ph]].
- [26] R. M. Francis, M. Frank and C. S. Kalman, Phys. Rev. D **43** (1991) 2369.
- [27] K. Huitu, J. Maalampi and M. Raidal, Phys. Lett. B **328** (1994) 60.
- [28] K. Huitu, J. Maalampi and M. Raidal, Nucl. Phys. B **420** (1994) 449.
- [29] K. S. Babu, S. M. Barr, Phys. Rev. **D48** (1993) 5354.
- [30] K. S. Babu, S. M. Barr, Phys. Rev. **D50** (1994) 3529.
- [31] M. Frank, H. Hamidian, K. Puolamaki, Phys. Lett. **B456** (1999) 179.
- [32] M. Frank, H. Hamidian, K. Puolamaki, Phys. Rev. **D60** (1999) 095011.
- [33] R. N. Mohapatra, hep-ph/9801235, and references therein.
- [34] K. Agashe, R. Contino, L. Da Rold and A. Pomarol, Phys. Lett. B **641**, 62 (2006).
- [35] K. Agashe, A. Delgado, M. J. May and R. Sundrum, JHEP **0308** (2003) 050.
- [36] R. N. Mohapatra and G. Senjanovic, Phys. Rev. Lett. **44** (1980) 912.
- [37] B. T. Cleveland, T. Daily, R. Davis, Jr., J. R. Distel, K. Lande, C. K. Lee, P. S. Wildenhain and J. Ullman, Astrophys. J. **496**, 505 (1998).
- [38] Y. Fukuda *et al.* [Super-Kamiokande Collaboration], Phys. Rev. Lett. **81**, 1562 (1998) [hep-ex/9807003].
- [39] R. N. Mohapatra and A. Rasin, Phys. Rev. Lett. **76** (1996) 3490.
- [40] R. N. Mohapatra and A. Rasin, Phys. Rev. D **54** (1996) 5835.
- [41] R. Kuchimanchi, Phys. Rev. Lett. **76** (1996) 3486 [hep-ph/9511376].
- [42] R. Kuchimanchi and R. N. Mohapatra, Phys. Rev. D **48** (1993) 4352 [arXiv:hep-ph/9306290].
- [43] K. Huitu and J. Maalampi, Phys. Lett. B **344** (1995) 217 [hep-ph/9410342].
- [44] C. S. Aulakh, A. Melfo and G. Senjanovic, Phys. Rev. D **57**, 4174 (1998) [hep-ph/9707256].
- [45] Z. Chacko and R. N. Mohapatra, Phys. Rev. D **58**, 015003 (1998) [hep-ph/9712359].
- [46] K. S. Babu and R. N. Mohapatra, Phys. Lett. B **668** (2008) 404.
- [47] M. Frank and B. Korutlu, Phys. Rev. D **83** (2011) 073007.
- [48] C. S. Aulakh, A. Melfo, A. Rasin and G. Senjanovic, Phys. Rev. D **58** (1998) 115007.

- [49] C. S. Aulakh, K. Benakli and G. Senjanovic, Phys. Rev. Lett. **79** (1997) 2188.
- [50] K. S. Babu, B. Dutta and R. N. Mohapatra, Phys. Rev. D **60** (1999) 095004.
- [51] G. Aad *et al.* [ATLAS Collaboration], Phys. Rev. Lett. **108**, 241802 (2012); G. Aad *et al.* [ATLAS Collaboration], Eur. Phys. J. C **72** (2012) 2244.
- [52] S. Chatrchyan *et al.* [CMS Collaboration], Eur. Phys. J. C **72** (2012) 2189.
- [53] K. Huitu, P. N. Pandita and K. Puolamaki, Phys. Lett. B **423** (1998) 97 [hep-ph/9708486].
- [54] S. Chatrchyan *et al.* [CMS Collaboration], arXiv:1402.4770 [hep-ex].
- [55] J. Abdallah *et al.* [DELPHI Collaboration], Eur. Phys. J. C **31**, 421 (2003) [hep-ex/0311019].
- [56] S. Chatrchyan *et al.* [CMS Collaboration], CMS PAS SUS-13-006.
- [57] D. A. Demir, M. Frank and I. Turan, Phys. Rev. D **73** (2006) 115001 [hep-ph/0604168].
- [58] J. N. Esteves, J. C. Romao, M. Hirsch, W. Porod, F. Staub and A. Vicente, JHEP **1201** (2012) 095 [arXiv:1109.6478 [hep-ph]].
- [59] M. Raidal, P. M. Zerwas, Eur. Phys. J. **C8** (1999) 479. [hep-ph/9811443].
- [60] M. Frank, K. Huitu, S. K. Rai, Phys. Rev. **D77** (2008) 015006. [arXiv:0710.2415 [hep-ph]].
- [61] D. A. Demir, M. Frank, K. Huitu, S. K. Rai and I. Turan, Phys. Rev. D **78**, 035013 (2008) [arXiv:0805.4202 [hep-ph]].
- [62] D. A. Demir, M. Frank, D. K. Ghosh, K. Huitu, S. K. Rai and I. Turan, Phys. Rev. D **79**, 095006 (2009) [arXiv:0903.3955 [hep-ph]].
- [63] A. Alloul, M. Frank, B. Fuks and M. R. de Traubenberg, Phys. Rev. D **88**, 075004 (2013) [arXiv:1307.1711 [hep-ph]].
- [64] K. S. Babu, A. Patra and S. K. Rai, Phys. Rev. D **88**, 055006 (2013) [arXiv:1306.2066 [hep-ph]].
- [65] A. Alloul, M. Frank, B. Fuks and M. Rausch de Traubenberg, JHEP **1310**, 033 (2013) [arXiv:1307.5073 [hep-ph]].
- [66] M. A. Shifman, A. I. Vainshtein, M. B. Voloshin and V. I. Zakharov, Sov. J. Nucl. Phys. **30**, 711 (1979) [Yad. Fiz. **30**, 1368 (1979)].
- [67] J. F. Gunion, H. E. Haber, G. L. Kane and S. Dawson, Front. Phys. **80**, 1 (2000).
- [68] A. Djouadi, Phys. Rept. **459**, 1 (2008) [hep-ph/0503173], Phys. Rept. **457**, 1 (2008) [hep-ph/0503172].
- [69] R. N. Cahn, M. S. Chanowitz and N. Fleishon, Phys. Lett. B **82**, 113 (1979).
- [70] L. Bergstrom and G. Hulth, Nucl. Phys. B **259**, 137 (1985) [Erratum-ibid. B **276**, 744 (1986)].
- [71] A. Djouadi, V. Driesen, W. Hollik and A. Kraft, Eur. Phys. J. C **1**, 163 (1998) [hep-ph/9701342].
- [72] C. -S. Chen, C. -Q. Geng, D. Huang and L. -H. Tsai, Phys. Rev. D **87**, 075019 (2013) [arXiv:1301.4694 [hep-ph]].
- [73] J. Beringer *et al.* [Particle Data Group Collaboration], Phys. Rev. D **86**, 010001 (2012).
- [74] M. Spira, Nucl. Instrum. Meth. A **389**, 357 (1997) [hep-ph/9610350].

- [75] A. Djouadi, J. Kalinowski and M. Spira, *Comput. Phys. Commun.* **108**, 56 (1998) [hep-ph/9704448].
- [76] A. Arhrib, R. Benbrik, M. Chabab, G. Moultaka and L. Rahili, *JHEP* **1204**, 136 (2012) [arXiv:1112.5453 [hep-ph]].
- [77] E. J. Chun, H. M. Lee and P. Sharma, *JHEP* **1211**, 106 (2012) [arXiv:1209.1303 [hep-ph]].
- [78] P. S. Bhupal Dev, D. K. Ghosh, N. Okada and I. Saha, *JHEP* **1303**, 150 (2013) [Erratum-ibid. **1305**, 049 (2013)] [arXiv:1301.3453].
- [79] ATLAS Collaboration, “Physics at a High-Luminosity LHC with ATLAS(Update),” Tech.Rep. ATL-PHYS-PUB-2012-004, CERN, Geneva, Oct, 2012.
- [80] CMS Collaboration, “CMS at the High-Energy Frontier. Contribution to the Update of the European Strategy for Particle Physics,” Tech.Rep. CMS-NOTE-2012-006, CERN, Geneva, Oct, 2012.